CAPITAL UNIVERSITY OF SCIENCE AND TECHNOLOGY, ISLAMABAD

Reduction of Reinforcement Using Jute Fiber Reinforced Concrete in Slabs under Impact Loading

by

Tasaddaq Hussain

A thesis submitted in partial fulfillment for the degree of Master of Science

in the

Faculty of Engineering
Department of Civil Engineering

2018

I want to dedicate this work to my family, who helped me throughout my education. This work is also dedicated to Armed Forces of Pakistan especially Pakistan Air Force for protecting the country from bad eyes of enemies.

CAPITAL UNIVERSITY OF SCIENCE & TECHNOLOGY
ISLAMABAD

CERTIFICATE OF APPROVAL

Reduction of Reinforcement Using Jute Fiber Reinforced Concrete in Slabs under Impact Loading

by

Tasaddaq Hussain

(MCE163017)

THESIS EXAMINING COMMITTEE

S. No.	Examiner	Name	Organization
(a)	External Examiner	Engr. Dr. Rao Arsalan Khushnood	NUST, Islamabad
(b)	Internal Examiner	Engr. Dr. Munir Ahmed	CUST, Islamabad
(c)	Supervisor	Engr. Dr. Majid Ali	CUST, Islamabad

Engr.Dr.Majid Ali
Thesis Supervisor
April, 2018

Engr. Dr. Ishtiaq Hassan
Head
Dept. of Civil Engineering
April, 2018

Engr. Dr. Imtiaz Ahmed Taj
Dean
Faculty of Engineering
April, 2018

Author's Declaration

I, **Tasaddaq Hussain** hereby state that my MS thesis titled "**Reduction of Reinforcement Using Jute Fiber Reinforced Concrete in Slabs under Impact Loading**" is my own work and has not been submitted previously by me for taking any degree from Capital University of Science and Technology, Islamabad or anywhere else in the country/abroad.

At any time if my statement is found to be incorrect even after my graduation, the University has the right to withdraw my MS Degree.

(Tasaddaq Hussain)

Registration No: MCE163017

Plagiarism Undertaking

I solemnly declare that research work presented in this thesis titled "**Reduction of Reinforcement Using Jute Fiber Reinforced Concrete in Slabs under Impact Loading**" is solely my research work with no significant contribution from any other person. Small contribution/help wherever taken has been dully acknowledged and that complete thesis has been written by me.

I understand the zero tolerance policy of the HEC and Capital University of Science and Technology towards plagiarism. Therefore, I as an author of the above titled thesis declare that no portion of my thesis has been plagiarized and any material used as reference is properly referred/cited.

I undertake that if I am found guilty of any formal plagiarism in the above titled thesis even after award of MS Degree, the University reserves the right to withdraw/revoke my MS degree and that HEC and the University have the right to publish my name on the HEC/University website on which names of students are placed who submitted plagiarized work.

(Tasaddaq Hussain)

Registration No: MCE163017

List of Publications

It is certified that following publication(s) have been made out of the research work that has been carried out for this thesis:-

Journal Article

1. Hussain, T., and Ali, M. (2018). Improving the Impact Resistance and Dynamic Properties of Jute Fiber Reinforced Concrete for Rebars Design by Considering Tension Zone of FRC. *Materiales de Construccin, (ISI Impact Factor =1.343, Under review).*

Conference Proceedings

1. Hussain, T., and Ali, M. (2018). Effectiveness of Jute Fiber in Concrete for Improving Impact Resistance of Slab. *3rd ACI FRC International Workshop*, Italy, June 2018 (Abstract accepted and paper submitted).

Tasaddaq Hussain
(MCE163017)

Acknowledgements

- I would like to thank Almighty Allah for his countless blessing.
- I am also grateful to my family for their continuous moral support.
- I would like to pay special gratitude to Engr. Dr. Majid Ali for his guidance and supervision, without which, this was not possible.
- I also want to thank Department of Civil Engineering for partial financial assistance.
- I am grateful to all who assisted me during this study especially Engr. Faisal Raza, Mr. M. Khalid, Mr. Syed Ali, Mr. M. Saqib, Mr. Nadeem Shehzad and Mr. M. Junaid for their kind help in lab work.

Abstract

The demand for the safety of structures against severe loading (e.g. impact) is increasing day by day. It becomes more important when it comes to the designing of important military/nuclear structures e.g. aircraft shelter. Structures safety is generally associated with the materials used for the construction. Concrete is main material used for construction but it is very weak in tension. To achieve economy without compromising the strength requirements, fibers are being used to enhance concrete's mechanical properties and impact resistance. However, the effectiveness of natural fibers in concrete under impact loading needs to be investigated in detail. In this study, behavior of jute fiber reinforced concrete (JFRC) under impact and dynamic loadings is experimentally investigated. The effectiveness of tension zone of fiber reinforced concrete (FRC) in reinforcement design is examined experimentally under impact loading. Small slab panels of plain concrete (PC) and JFRC, without and with steel reinforcements, are tested for flexural strength and impact resistance. Simplified drop-weight test is used to find the impact resistance in laboratory. Reinforcement in slab is designed using tension zone of FRC and its value is compared with ACI design. Dynamic elastic modulus, resonance frequencies and damping ratios are found for different specimens as per ASTM standard. Basic mechanical properties are also determined. Cracking behavior of specimens under different tests is observed. Fracture surface is examined at micro level through scanning electron microscope (SEM) under impact and flexure loads. Significant improvement in impact resistance of concrete is seen by incorporation of jute fibers. Impact resistance of JFRC is enhanced up to 6 times as compared to PC. Dynamic elastic modulus and damping ratio are also enhanced by 68% and 100%, respectively. Flexure and split-tension strengths are increased by 20% and 8%, respectively. It is concluded that about 30% steel reinforcement in slabs can be reduced by the use of short jute fibers in concrete.

Contents

List of Figures

List of Tables

Abbreviations

CE_m	Compressive energy absorption up to maximum load
CE_u	Compressive energy absorption from maximum load to ultimate load
CE	Compressive total energy absorption
CT	Compressive toughness
E_d	Elastic dynamic modulus
f_c	Compressive strength
f_f	Flexure strength
f_L	Longitudinal frequency
f_r	Rotational/torsional frequency
f_s	Split tensile strength
f_t	Transverse frequency
FE_m	Flexure energy absorption up to maximum load
FE_u	Flexure energy absorption from maximum load to ultimate load
FE	Flexure total energy absorption
FT	Flexure toughness
FRC	Fiber reinforced concrete
IR	Impact resistance
IFS	Impact fist crack strength
IUS	Impact ultimate strength
JF	Jute fiber
JFRC	Jute fiber reinforced concrete
JFSRC	Jute fiber steel reinforced concrete
kN	kilo-Newton
kJ	kilo-Joule

l_f	Length of fiber
v_f	Volume fraction
mm	Millimeter
MPa	Mega Pascal
PC	Plain concrete
Pm	Maximum load
Pu	Ultimate load
PRC	Plain reinforced concrete
s	Second
SE	Split total energy absorption
SEM	Scanning electron microscope
SE_m	Split energy absorption up to maximum load
SE_u	Split energy absorption from maximum load to ultimate load
ST	Split toughness
w/c	Water cement ratio

Symbols

Δ_f	Deflection under flexure
Δ_i	Deflection under impact
Δ_{i60}	Deflection under impact height of 60 cm
Δ_{i90}	Deflection under impact height of 90 cm
δ	Strain
ξ	Damping ratio
Φ	Diameter of fiber

Chapter 1

Introduction

1.1 Background

The behavior of slabs under impact loading is an important issue to investigate. Its importance increases when it comes to structures that are designed to survive accidental loading and structure exposed to high threats such as military/nuclear structures (Hrynyk and Vecchio 2014). Aircraft shelter is one of the important military structure. It is often expected to encounter a missile or rocket attack. When a missile strikes on aircraft shelter, it will collapse as shown in the figure 1.1 (b). Falling rocks and debris flows are some common mode of impact loads which are often faced by different structures. Structure safety during such type of loading is mainly dependent on its impact resistance (IR). IR is the capability of concrete to resist sudden load without cracking (Muda et al. 2016). Enhanced IR and maximum energy absorption are the desired properties in concrete. In the recent times, researches are being done to enhance the impact resistance of structures. Keeping in view the importance of impact resistance, ACI has reported different methods to find IR of concrete and concrete based composites in laboratory. Among all methods, drop-weight test is the simplified test and can be used to generate impact load in laboratory to find impact resistance. Impact resistance can be related to: i) energy absorb to rupture a specimen, ii) number of blows to achieve predefined degree of failure in drop-weight test, iii) magnitude of damage. Number of blows in drop-weight test can also be used for relative comparison of IR of different specimens (ACI 544.2). Sometimes, dynamic loading is also associated with impact load. Structures usually faces severe dynamic loading due to impact. For example, vehicle crash impact, missile or aircraft impact and shock and explosion impact (Zineddin and Krauthammer, 2007). Hence, behavior under impact and dynamic loadings need to be explored.

(a) (b)

FIGURE 1.1: Aircraft shelter: a) before impact and b) after impact.

1.2 Research Motivation and Problem Statement

The demand for the safety of structures against severe loading (e.g. impact) is increasing day by day. This requires manufacturing of high-performance materials having superior mechanical properties. But economy of structures should not be compromised. Fibers are being used for enhancing the concrete's resistance to impact loading. Hence, the problem statement is as follows:

"Construction of structures having better resistance to severe dynamic/impact loading is of great concern. Structures safety is associated with the materials used for construction. Concrete is main material used for construction but it is very weak in tension. Tension of concrete is controlled by providing steel reinforcements but it becomes little expensive. To achieve economy without compromising the strength requirements, fibers are being used which enhances concrete's mechanical properties and impact resistance. Impact resistance of concrete can be enhanced

by using jute fibers. There are few researches for the improvement of impact resistance of concrete but no one addresses the possible reinforcement reduction due to enhanced properties of jute fiber reinforced concrete (JFRC)".

1.3 Objective and Scope of Work

The overall goal of this research program is to economically manufacture a concrete having better impact resistance and mechanical properties.

The specific objective of this research is to reduce reinforcement in slabs using jute fiber reinforced concrete under impact loading along with determination of mechanical and dynamic properties.

To achieve this objective, scope of work is defined as follows:

i. Mechanical properties to be determined are compressive strength, split-tension strength, flexural strength, energy absorption, toughness.

ii. To find the impact resistance, drop-weight test is used.

iii. Resonance frequencies are found to determine the dynamic elastic modulus and damping ratio.

iv. SEM analysis of JFRC specimens will be used to determine the failure mechanisms and bonding of jute fibers.

v. Based on experimental results, empirical equations will be predicted to determine impact resistance.

vi. Economical reinforcement design of slab will also be suggested by utilizing tension zone of FRC.

1.4 Methodology

In this experimental study, the mechanical properties of PC and JFRC will be determined in lab. The mix design ratio for PC is 1:3:2:0.7 (cement: sand: aggregate: water). 5 cm long jute fibers with a fiber content of 5% by mass of cement are used for preparing JFRC. The mix design for JFRC is same as that of the PC. The standard specimens are cast and tested for determining the compressive, flexural and split- tension strength. Slab panel of size 11"×17"×3" arel cast and tested for flexural strength, energy absorption and impact resistance of PC and JFRC. Resonance frequencies of all cast specimens are also be determined.

1.5 Thesis Outline

There are six chapters in this thesis, which are as follows:

Chapter 1 consists of introduction section. Importance of impact resistance is explained in this chapter. It also consists of research motivation and problem statement, objective and scope of work, methodology and thesis outline.

Chapter 2 contains the literature review section. It consists of background, improvement in impact resistance of concrete by using fibers, improvement in mechanical properties of concrete by using fibers, reinforcement design of slab and summary.

Chapter 3 consists of experimental program. It contains background, ingredients, concrete preparation procedure, specimens' details, testing procedures and summary.

Chapter 4 consists of experimental evaluation. It contains background, results of testing for mechanical properties (i.e. compressive, split-tension and flexure strength, behavior and energy absorption), impact testing, resonance testing, SEM analysis and summary.

Chapter 5 comprises of discussion. It is divided into background, relationship of impact resistance with mechanical properties, empirical equations, reinforcement design and summary.

Chapter 6 includes conclusion and recommendations.

Bibliography is presented right after chapter 6.

Annexures are given at the end. Annexure A explains the results from the testing of mechanical properties of remaining specimens. Annexure B explains the results from the testing of impact resistance of remaining specimens. Annexure C consists of remaining SEM images.

Chapter 2

Literature Review

2.1 Background

Fibers are used to enhance concrete's toughness and mechanical properties since ancient time. Fiber reinforced concrete (FRC) has proved to have better fracture/flexural toughness and impact resistance. It also shows better performance to static as well as dynamic loading. It is the need of the time to explore the effectiveness of natural fibers for enhancing impact resistance. As natural fibers are cheap and environment friendly. Jute fiber is one of the natural fiber which is widely produced in South Asian countries. Furthermore, impact resistance is an important issue to investigate. There is no well-established standard to find impact resistance but many researches are done to draw a comparative analysis of impact resistance of different materials.

2.2 Improvement in Impact Resistance of Concrete by Using Fibers

Many researches are done on improvement of impact resistance through FRC. Different procedures were adopted by different researcher to assess the impact resistance. As there is no standard for experimentally evaluating the impact resistance of specimen. Rahacek et al. (2013) specified two test methods to find impact resistance. First method is a dynamic test in which load is applied at a rate of 70 mm/s. This high loading rate will act like impact load. Second method specified was drop-weight test. A weight of 9.5 kg is dropped on specimen and number of blows were noted till failure. Concrete reinforced with steel fiber were examined under both methods and improvement in the impact resistance is found as compared to plain concrete. Ueno et al. (2016) evaluated concrete plates enriched with polypropylene fibers under high velocity impact. It was found that polypropylene fibers reinforced concrete (PPFRC) has more compressive dynamic strength and fracture energy as compared to PC. Local failure with scabbing of concrete was observed in PPFRC plates under impact test. Eftekhari & Mohammadi (2016) investigated the dynamic behavior of concrete reinforced with carbon nano-tubes (CNT) under a projectile. It was found that the CNT-reinforced concrete had less deteriorated area under projectile load. It had more impact resistance and absorbed energy. Less penetration depth of high velocity projectile was observed in CNT-reinforced concrete. Hrynyk and Vecchio (2014) investigated the SFRC slabs under impact loadings. Slabs of size 180×13×13 cm with varying longitudinal reinforcements and steel fibers were tested under drop-weight test. Improved impact resistance and reduced crack spacing and width was resulted by the incorporation of steel fibers. Shear failure was also overserved in slabs contrasting to flexural failure for which it was designed. Ulzurrun and Zanuy (2017) tested beam reinforced only with longitudinal reinforcements under drop-weight load. It was observed that SFRC beams failed due to flexural as compared to PC beams which failed due to shear. As compared to synthetic fibers, natural fibers are also being used as reinforcing materials in mud and cement-based composites since ancient times. They are also very economical as compared to synthetic fibers. Wang and Chouw (2017) investigated the effect of coconut fibers on impact resistance of concrete. Cylinders of size 20×10 cm were tested under single and multiple drop-weight tests. Change in elastic modulus of coconut fiber reinforced concrete (CFRC) was evaluated under single drop test. Effect of variable drop height on compressive strength and failure mechanism was investigated under multiple drop heights. Reduced spalling of concrete was observed in CFRC as compared to PC. It was found that increasing the impact height, increases the compressive strength of CFRC. Different failure mechanism was observed under static and impact loading. Zhou et al. (2013) investigated the fracture and impact properties of jute fiber reinforced cementitious composites (JFRCC). Mortar (not concrete) slabs panels of size 20×20×2 cm were tested under drop weight test. It was found that JFRCC had absorbed more blows of drop weight until failure as compared to plain concrete. This indicates the improvement in the impact resistance of concrete due to incorporation of short jute fibers. This study lacks in practical point of view as it did not consider the steel reinforcement and concrete.

2.3 Improvement in Dynamic Properties of Concrete by Using Fibers

Fibers are also being used for the enhancement in the dynamic properties of concrete. Yan and Chouw (2013) investigated the dynamic properties of coir fiber reinforced concrete (CFRC) cylinders, without and with flax fiber reinforced polymer (FFRP) tube confinement. Specimens were tested as per ASTM C215 to determine the resonance frequencies, dynamic elastic modulus and damping ratios. Decrease in the resonance frequencies and dynamic elastic modulus of unconfined CFRC was found as compared to PC. But damping ratios of unconfined CFRC were increased significantly as compared to PC. Increment of about 280-362% in the damping ratio of CFRC is observed. Giner et al. (2012) investigated the dynamic properties of steel and carbon fiber reinforced concrete containing silica fume. ASTM C215 was used to find the resonance frequencies of prismatic specimens. Dynamic elastic modulus and damping was also found. It was found that frequencies increased by incorporation of carbon fibers but decreased by incorporation of steel fibers. Dynamic elastic modulus had also shown similar trend.

Table 2.1: Characteristic of different impact loads used by different researchers.

Apparatus Type	Impact Height/Velocity	Impact Weight	Specimen Size (mm)	Output	Reference
Instrumented Drop-weight	10/20 cm	9.5 kg	700×300×50	Strength (blows)	Rahacek et al. (2013)
Simple Drop-weight	24.7 cm	14 kg	120 mm^3	Strength (blows)	Amusan et al (2017)
Instrumented Drop-weight	1.75 m	200 kg	125×250×2000 (Beam)	Strength (kN) and energy absorption (kN.m)	Ulzurrun and Zanuy (2017)
Steel projectile	190-420 m/s	46 g	500×500×60/80 (Plates)	Strain, penetration depth (mm) and spalling diameter (mm)	Ueno et al. (2016)
Projectile	400m/s		300×250 mm	Penetration depth (mm)	Eftekhari and Mohammadi (2016)
Instrumented Drop-weight	3.26 m	150-300 kg	1800×130×130 (Slab)	Displacement (mm) and reaction (kN)	Hrynyk and Vecchio (2014)
Instrumented Drop-weight	40/60 cm	40 kg	200×100 mm (Cylinder)	Force (kN) and strain	Wang and Chouw (2017)

Increment in the damping of concrete is also found by incorporation of carbon fiber. In contrast to carbon fiber, damping reduced due to addition of steel fibers. Ali et al. (2012) also examined the dynamic properties of coconut fiber reinforced concrete. Fundamental frequencies, dynamic elastic modulus and damping ratios were found. These properties were found at different damages stages by repeatedly applying the small impact load. Increment in the damping of coconut fiber reinforced concrete was seen as compared to plain concrete while decrement in the frequencies was also observed. Damping was increased by increasing the fiber content and increment was more prominent with the increase in cracking. It was reported that more cracked section would result more damping. Furthermore, dynamic elastic modulus of coconut fiber reinforced concrete was reduced as compared to static elastic modulus. There was a difference of 7% in the dynamic and static elastic modulus. Elastic modulus also tend to decrease with the increment in the fiber content.

2.4 Improvement in Mechanical Properties of Concrete by Using Fibers

Jute fiber are being used in concrete to enhance its mechanical properties since long time. Aziz and Mansur (1988) reported that JFRC can be an effective and economical material for building construction especially in South Asian countries. Zakaria et al. (2017) studied the effect of jute fiber as reinforcing material in concrete. Specimens of standard size were tested for flexure, compressive and tensile strengths. Significant improvement in the mechanical properties was observed by the incorporation of jute fibers. This indicates that jute fiber reinforced concrete (JFRC) can be an effective material for low cost construction. Zia and Ali (2017) studied the effect of different fiber for reducing the cracks in canal lining. Behavior of jute fiber reinforced concrete (JFRC), nylon fiber reinforced concrete (NFRC) and polypropylene fiber reinforced concrete (PPFRC) was examined for compression, flexure, split tension and shrinkage. Cylinders and prisms of standard size

Table 2.2: Fiber content, mix design and fiber length used by different researchers for preparing JFRC

Fiber Content	Mix Design ratio	Fiber Length (mm)	References
0.1,0.3, 0.5%*	1 : 2.77 : 2.46	20	Razmi and Mirsayar (2017)
5%**	1 : 3 : 1.5	50	Zia and Ali (2017)
0.6 kg/m^3	1 : 1.74 : 3.24	30	Liu et al. (2013)
1%**	1 : 1.5 : 3	40	Chandar and Balaji (2015)
4.4 kg/m^3	1 : 1.5 : 2.7	50	Kundu et al. (2012)
0.25, 0.50%**	1 : 1.5 : 3	15	Zakaria et al. (2016)
0.25, 0.50%**	1 : 2 : 4	15	

*Note: * content by weight of mix, ** content by mass of cement, *** content by volume fraction of concrete.*

were tested. Significant improvement in the energy absorption and toughness of JFRC is observed with respect to PC. Furthermore, water absorption of JFRC was also increased by 8%. It was concluded that cracks could be significantly reduced by using fibers in concrete.

Different mix designs were used by different researchers to prepare JFRC with different fiber contents and lengths as shown in Table 2.2. Kundu et al. (2012), Liu et al. (2013), Chandar and Balaji (2015) and Zakaria et al. (2016) followed the conventional mix design approach in which content of coarse aggregates was double as compared to that of sand. To provide adequate sand for grabbing fibers, Zia and Ali (2017) used more sand content (double) as compared to coarse aggregates.

2.5 Scanning Electron Microscopic Analysis

Failure surfaces of specimens are analyzed through scanning electron microscope to study the interfacial bonding of fiber and concrete matrix. Atahan et al. (2013) investigated the behavior of fiber reinforced cementitious composites (FRCC) specimens under different types of test through SEM. Polyvinyl alcohol (PVA) fibers were used with different volume fractions to make FRCC. The fractured surfaces were examined through SEM under flexure and impact test. Specimen has shown different failure mechanism under flexure and impact test. Fiber pullout was prominent under impact load. Same failure mechanism was also seen under impact and static load when low volume fraction of fiber is added. But more fibers were pulled out under impact load as compared to static flexure load. Tai et al. (2016) examined the effectiveness of steel fiber reinforced ultra-high performance concrete under different pull out rates. Failure surfaces of specimens were examined through SEM after quasi-static and impact tests. Different failure behavior was seen under static and impact loads. Under quasi-static load, cracks were produced near fiber surface but in case of impact load, breakage of aggregates occurred. Surface morphology of the hybrid composites made of jute and coir fiber was one of the studied feature by Saw et al. (2014). Microstructure of jute and coir fibers were examined through SEM. Nano strands/threads of the jute fiber were closely bonded due to the presence of intercellular ingredients. These small intercellular ingredients were equally spread throughout the fiber matrix. Adjacent placements of the threads were the reason for the better strength of jute fiber. Failure surfaces of hybrid composites were also examined under tensile load. Jute fibers was well immersed in epoxy which resulted in strong bonding of jute fiber and composite's matrix. Due to strong bonding of jute fiber, less fiber pulled out was observed. There was more fiber breakage.

2.6 Reinforcement Design of Slab

Steel reinforcement is normally expensive among all materials used in construction of slabs. Economy can be achieved if amount of steel reinforcements can be reduced either by enhancing the tensile concrete's strength or by increasing the slab thickness. ACI slab design is based on Whitney (1942) stress strain diagram shown in Figure 2.1(a). The effect of concrete in tension zone is neglected due to its low magnitude. But Beshara et al. (2012) reported that the effect of FRC in tension zone should not be neglected. Whitney stress strain diagram was modified to incorporate the effect of FRC in the tension side and new design equation was proposed. Modified stress strain diagram is shown in Figure 2.1(b).

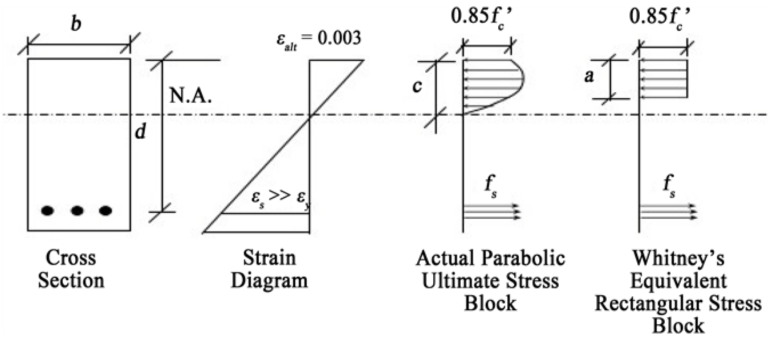

(a)

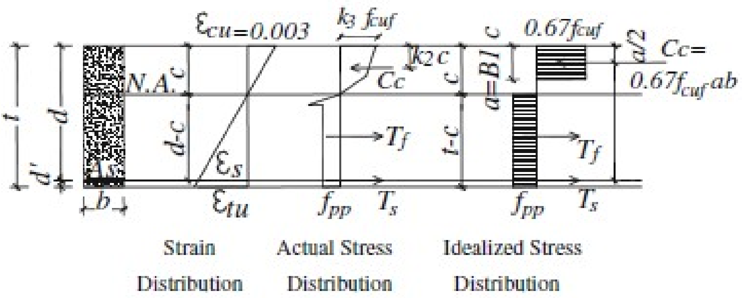

(b)

Figure 2.1: Stress Strain Diagram: a) Whitney 1942 and b) Beshara et al. 2012.

Modified design equation proposed by Beshara et al. (2012) for fiber reinforced concrete is given below:

$$M_n = \rho bdf_y(d - \beta c/2) + T_f[(d + c - \beta c)/2] \tag{2.1}$$

Where $T_f = 1.64v_f(l_f/\Phi)bt_f$ (Can be directly obtained from experimental results), t_f = tensile strength of fiber, v_f = volume fraction and l_f/Φ = aspect ratio of fiber. The equation was verified through experimental testing of beam under static flexure load.

There are two options to use Beshara et al. equation for the design of slabs under impact load. First option is to convert impact load to static load and found moments through static formula. Second option is to directly find moment due to impact load. Pham and Hao (2016) presented a bending moment diagram (BMD) and formula to calculate moment under impact loading. Proposed BMD is shown in Figure 2.2. Hence moment can simply be calculated by the following formula proposed by Pham and Hao (2016).

$$M = \frac{P}{L(1 - 4a^2/L^2)} \left(\frac{L^2}{12} - a^2 - \frac{4a^3}{3L} \right) \tag{2.2}$$

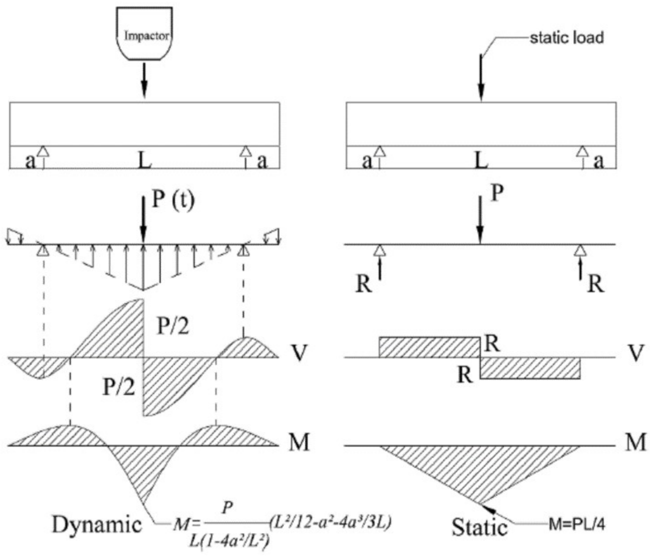

FIGURE 2.2: Bending moment diagram under impact and static load (Pham and Hao 2016).

2.7 Summary

It is well evident from the literature review that fibers can be used to enhance the impact resistance. Most of the researches are done on synthetic fibers. Synthetic fibers are normally expensive as compared to natural fibers. Secondly, natural fibers are environment friendly. Among all natural fibers, only coconut fibers in concrete (Wang and Chouw 2017) and jute fibers in mortar (Zhou et al. 2013) were used for impact resistance. The behavior of jute fibers in concrete under impact loading still needs investigation. Steel rebar design has not been reported by taking impact load and FRC's tension zone into consideration so far. As per authors' knowledge, no research is conducted on JFRC slabs for impact resistance and reinforcement reduction in slabs at the same time. Slabs of PC, PRC (PC with steel rebars), JFRC and JFSRC (JFRC with steel rebars) are tested under impact and flexure load. Cylinders are also tested for dynamic properties (i.e.

dynamic elastic modulus, resonance frequencies and damping ratio) and basic mechanical properties (i.e. compression and split-tension strength). Scanning electron microscopic analysis is also performed to examine the interfacial bonding and failure mechanism of jute fibers in concrete.

Chapter 3

Experimental Program

3.1 Background

Use of fibers for enhancing the mechanical properties and impact resistance is increasing day by day. Increased flexure strength, toughness and energy absorption are the main advantages of fiber reinforced concrete. Effectiveness of jute fiber for enhancing the impact resistance is explored through the experimental work. In this chapter ingredients, concrete preparation procedure, specimens' details and testing procedures are explained in detail.

3.2 Ingredients

For the preparation of plain concrete, ordinary Portland cement, local sand, normal size aggregate and drinking water are used. For preparing JFRC, same ingredient with addition of jute fibers (JF) having 50 mm length and 0.5 mm diameter are used. JF are manually cut to the desired length of 50mm. Microstructure of jute fiber is examined through scanning electron microscope. SEM images of single jute fiber are presented in Figure 3.1.

It can be noted that jute fiber consists of nano strands which are laid together in longitudinal direction (refer to Figure 3.1 (b)). By looking at the edge of fiber, it can be seen that these nano strands are empty. This can be the source of water absorption capacity of jute fiber. Ø6 steel rebars of grade 40 are also used for preparing PRC and JFSRC slabs.

(a)

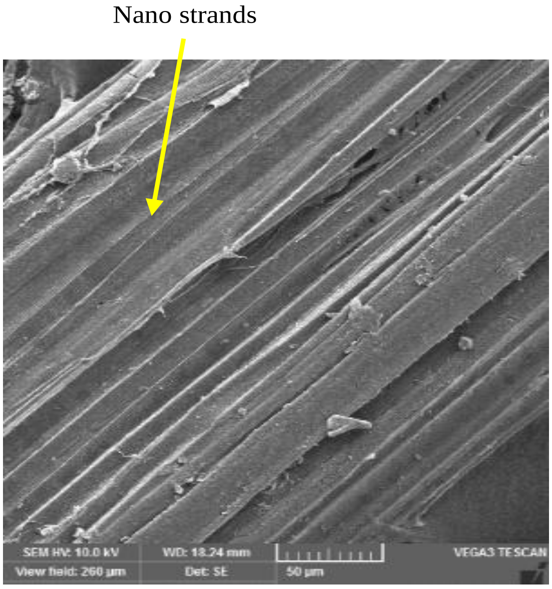

(b)

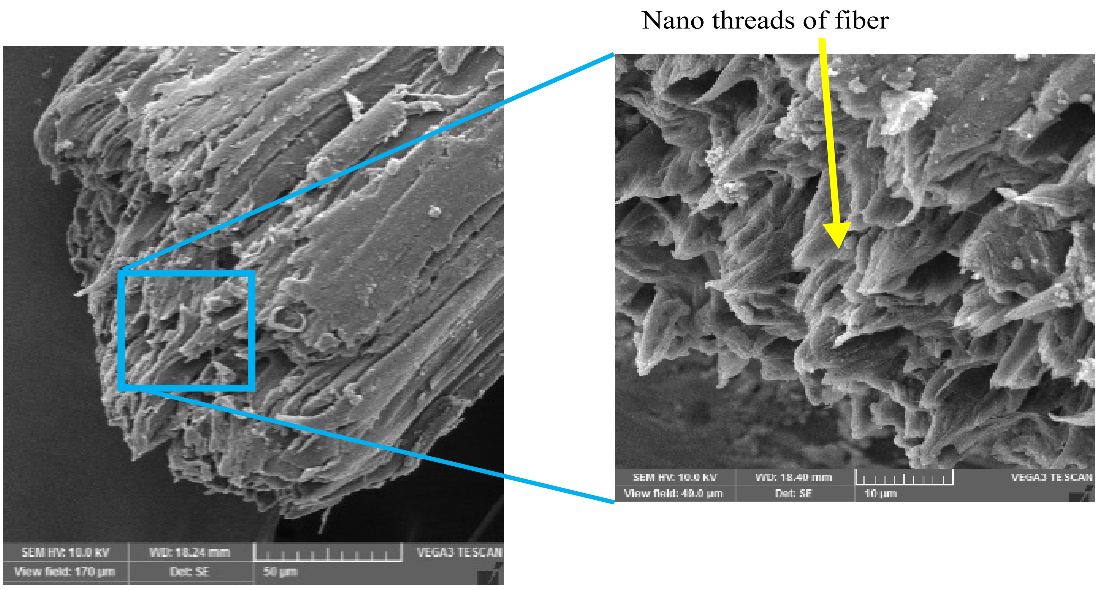

(c)

FIGURE 3.1: Jute fiber: a) Naked eye view, b) Top surface @ 50μm and c) Edge of fiber @ 50μm.

3.3 Concrete Preparation

Cement, sand, aggregate and water with a ratio of 1:3:2:0.7, respectively, are used for preparing plain concrete. 50 mm long jute fibers with a content of 5%, by mass of cement, are used for preparing JFRC. The mix design for JFRC is the same as that of the PC. More ratio of sand is used in mix design to provide more mortar for grabbing the fibers and to get proper mixing of fibers in the matrix. High water-cement ratio is used to make reference (PC) and desired (JFRC) materials of same mix design for comparison purpose. It may also be noted that w/c ratio is high due to high content of sand creating more surface areas of materials used. Furthermore, strength is not targeted. Main emphasis is high damping and impact resistance using fibers in concrete. No considerable bleeding is observed in PC and JFRC during slump test and filling of molds. Generally, a mix design of 1:2:4 is used for concrete, but to provide adequate sand for grabbing fibers in JFRC, Zia and Ali (2017) used more sand content (double) as compared to coarse aggregates. Thus, a mix design of 1:3:1.5 with jute fiber content of 5% by mass of cement, was selected. However, compressive strength was compromised due to low content of aggregates. In order to improve compressive strength and keeping in mind the grabbing of fibers, a mix design of 1:3:2 (i.e. a little more aggregates in comparison to mix design of Zia and Ali 2017) is considered in this study.

Plain concrete is prepared in drum type mixer. The mixer was rotated for six minutes after putting all materials in the mixer along with the water. For preparing JFRC, a different approach, reported by Chakraborty et al. (2013), is adopted. First of all, jute fibers are soaked in water for 24 hours. Then, fibers are left open in air for 30 minutes before mixing. After that, materials are put in the mixer layer by layer to prevent from balling effect. One third part of aggregate, sand, cement and jute fibers are spread into the mixer. Same procedure was repeated until the complete materials are placed into the mixer. After complete placing of materials into the mixer, approximately 1/3 water is spread on all ingredients. Mixer is started and remaining water is added. Mixer is rotated for six minutes to get uniform concrete. Before casting of molds, slump of PC and JFRC is found.

JFRC has less slump as compared to PC. This is due to more water absorption capacity of jute fiber. There is difference of 30 mm among slump values of PC and JFRC. This difference could be more but it is less due to the prior immersion of jute fibers in water. Due to immersion, jute fibers have absorbed comparatively less water. Slump of JFRC is reduced by 60% as compared to PC. Molds are casted by spreading the concrete in three layers and tamping each layer 25 times with rod. Molds of PC and JFRC are prepared by same procedure instead of lifting-dropping technique used by Khan and Ali (2016) and Ali et al. (2012). This is possible only because fibers are immersed in water and dried before mixing. Following this procedure, minimized the water absorption of jute fiber, resulted a workable JFRC. After two days' specimens were demolded and placed into curing tank for 28 days. Prior to testing, densities of PC and JFRC are found by dividing the weight of specimen with its volume. A decrease in the density of JFRC is observed. This is due to the low unit weight of jute fibers. JFRC is 20% less dense than PC.

3.4 Specimen

The detail of specimens prepared is given in Table 3.1. Slab panels of size 430×280×75 mm are prepared for PC and JFRC for flexure and impact test. A set of six samples for batch of PC and JFRC are produced for flexure test. Out of six, three samples have steel rebars of Ø6@100 mm. Similarly, ten samples are prepared for impact test for each impact heights of 60 and 90 cm and batch of PC and JFRC. Out of ten, five samples have steel rebars of 6 mm diameter for both impact heights. Six cylinders of 10 cm diameter and 20 cm height are also prepared for compression and split-tension testing from batch of PC and JFRC. A total of 52 slabs and 12 cylinders are cast. Notation of PC is used for plain concrete, PRC for plain concrete having steel rebars, JFRC for jute fiber reinforced concrete and JFSRC for jute fiber reinforced concrete having steel rebars. A minimum of three readings is taken for basic mechanical properties (compression, flexure, and split-tension). A minimum of five readings is taken for impact resistance and resonance properties (dynamic elastic modulus, damping ratio and fundamental frequencies).

Table 3.1: Detail of specimens prepared.

PC **1:3:2:0.7**	**JFRC** **1:3:2:0.7 (5 cm long jute fibers with 5% by mass of cement)**	**Properties determined**
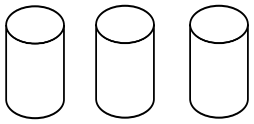	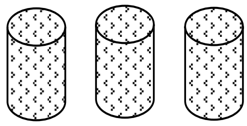	▪ Compressive strength and Strain ▪ CE_m, CTE, CT ▪ Cracking behavior
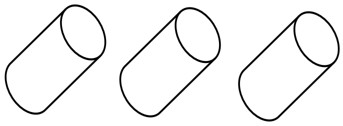	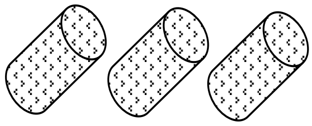	▪ Split tensile strength ▪ SE_m, STE, ST ▪ Cracking behavior
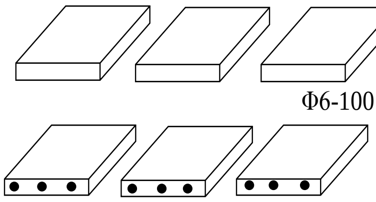 Φ6-100 mm	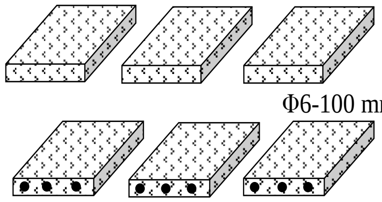 Φ6-100 mm	▪ Flexure strength ▪ FE_m, FTE, FT ▪ Load-deflection curve ▪ Cracking behavior
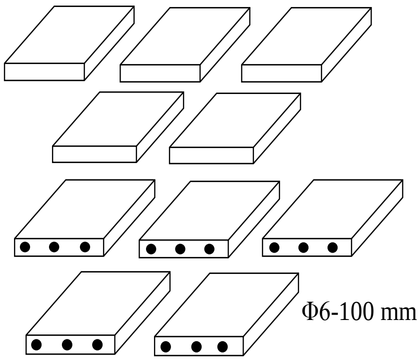 Φ6-100 mm	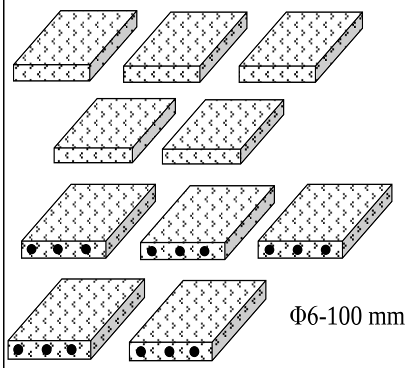 Φ6-100 mm	**Impact Height = 60cm** ▪ Impact first crack strength ▪ Impact ultimate strength ▪ Deflection ▪ Rebar design ▪ Cracking behavior
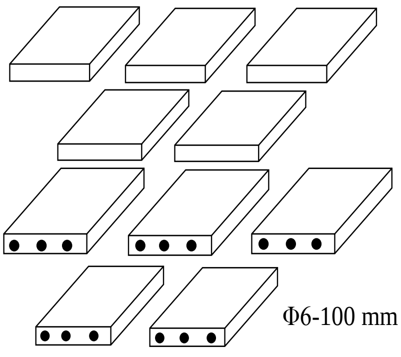 Φ6-100 mm	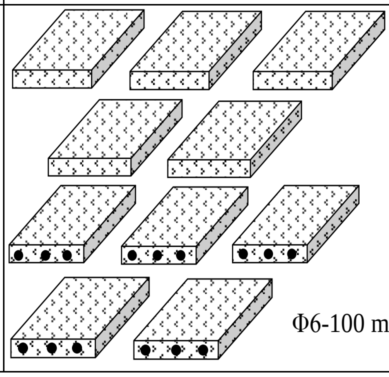 Φ6-100 mm	**Impact Height = 90cm** ▪ Impact first crack strength ▪ Impact ultimate strength ▪ Deflection ▪ Rebar design ▪ Cracking behavior

Note: Cracking behaviour is analysed for all specimens. SEM analysis is performed for selected JFRC specimens under each load.

3.5 Testing Procedure

Compressive strength and corresponding strain, split-tension strength and corresponding load-time curve, flexural strength and corresponding deflection, impact resistance and corresponding deflection, resonance frequencies, dynamic elastic modulus and damping ratio are found. Fracture surface of specimens is also examined at micro level through scanning electron microscope (SEM) under impact and flexure tests. SEM analysis is used to study the facial bonding of jute fibers and concrete matrix.

3.5.1 Testing for Mechanical Properties

3.5.1.1 Compression Strength (f_c)

PC and JFRC's cylinders are tested as per ASTM C39 in servo-hydro testing machine (STM) to find compressive strength and corresponding strain. From the test results, stress strain curve is obtained. Compressive energy absorption and toughness are also calculated from stress-strain curve.

3.5.1.2 Split-tension Strength (f_s)

Cylinders of standard size of PC and JFRC are tested in servo-hydro testing machine (STM) for split-tension as per ASTM C496 to get load-time curve. Split-tension energy absorption and toughness are calculated from load-time curve.

3.5.1.3 Flexure Strength (f_f)

ASTM C 293 is followed to find flexural strength and corresponding deflection of slabs of PC, PRC, JRFC and JFSRC. Specimens are tested in servo-hydro testing machine (STM). Load-deflection curve is used to find flexural energy absorption and toughness.

3.5.2 Impact Resistance (IR)

Slabs of PC, PRC, JRFC and JFSRC are tested under drop-weight test to find impact resistance. A simplified apparatus is developed to find IR in lab. Schematic diagram and experimental test setup are shown in Figure 3.2.

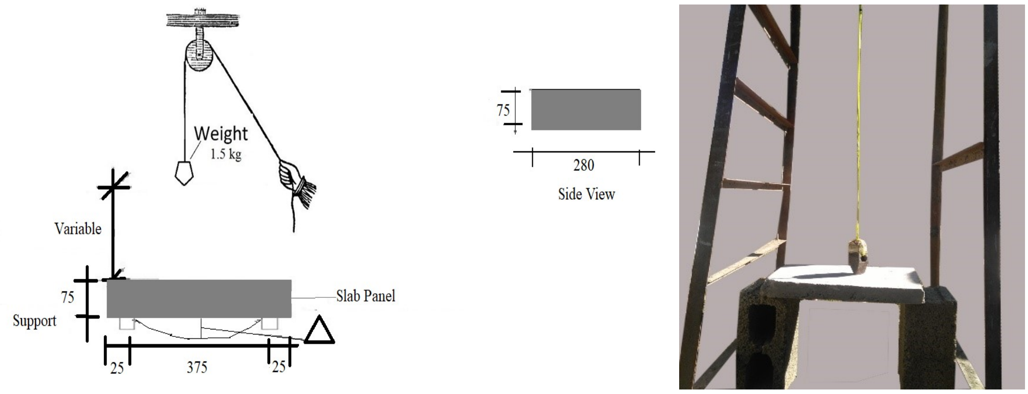

(a) (b)

FIGURE 3.2: Experimental impact testing. a) Schematic diagram and b) Test set up.

This apparatus gives results as per the requirements of ACI and test methods specified by Rahacek et al. (2013). A weight of 1.5 kg is dropped from variable heights and crack propagation is observed. Drop heights of 60 and 90 cm are used. Numbers of blows of drop-weight to first crack and failure are noted. Failure of specimen is considered when a complete crack is developed throughout the cross section of specimen. This is insured when a crack which started from bottom surface reaches at top surface and visible by naked eye. Deflection at the time of failure is also measured.

3.5.3 Dynamic Properties

All prepared specimens i.e. cylinders and slabs are tested as per ASTM C215 to find resonance frequencies. Specimens are tested at two stages, first before any test and second after test. Specimens that are not broken into pieces after tests are tested only. Longitudinal, transverse and torsional/rotational frequencies are found under impact resonance method. Dynamic elastic modulus and damping ratios are also found.

3.5.4 SEM Analysis

Fracture surfaces of specimens at micro level are examined through scanning electron microscope. SEM images are taken for specimens under different test i.e. flexure and impact tests for identification of fiber bonding and failure mechanism.

3.6 Summary

PC Specimens are prepared for a mix design of 1:3:2:0.7. 5% Jute fiber by mass of cement is added to prepare JFRC with same mix design. Ø6@100 mm reinforcement are also added in specimen to prepare PRC and JFSRC. A total of 52 slab panels of PC, PRC, JFRC and JFSRC are tested for flexure and impact loading. 1.5 kg drop-weight is used to find impact resistance with drop heights of 60 and 90 cm. 12 cylinders are also tested to find compressive and split-tension strength. All specimens are also tested to find dynamic elastic modulus and damping ratios.

Chapter 4

Experimental Evaluation

4.1 Background

Mix design of 1:3:2:0.7 (cement: sand: aggregate: w/c) is used for preparing PC. JFRC is prepared with same mix design except 5 cm long jute fiber are added by 5% mass of cement. Ø6@100 mm reinforcement are also added in specimen to prepare PRC and JFSRC. Evaluation of experimental results performed on PC, JFRC, PRC and JFSRC are discussed in this chapter.

4.2 Testing for Mechanical Properties

4.2.1 Compressive Strength, Behavior and Energy Absorption

Figure 4.1 (a) shows the behavior of specimens and developments of cracks. Stress-strain curves for PC and JFRC are presented in Figure 4.1 (b). At 99% of the maximum load of PC, first crack is developed. However, in case of JFRC, first crack is seen at 88% of the maximum load. Crack in JFRC is very tiny in both width and length as compared to the crack in PC. Number and size of cracks increases significantly at the maximum load for PC as compared to JFRC, which has less cracks.

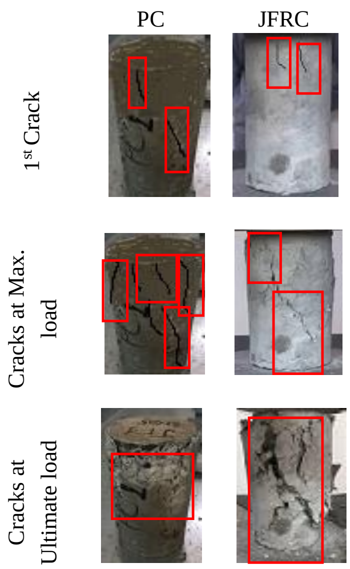

(a)

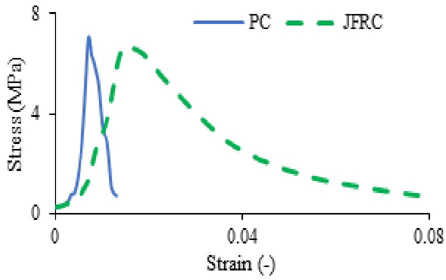

(b)

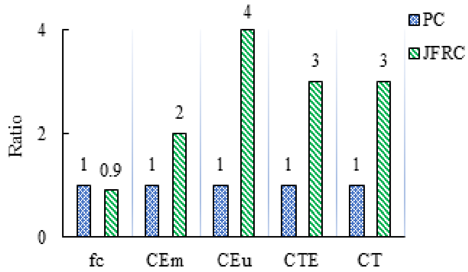

(c)

FIGURE 4.1: a) Compressive cracking behavior, b) compressive stress-strain curve and c) compressive strength, energy absorption and toughness index ratios.

At the ultimate stage, some fragments of concrete are fallen from the top of PC specimen. However, JFRC has only observed increase in cracks numbers and sizes. Better performance of JFRC is due to the bridging of jute fibers. To know the fiber's failure mechanism, JFRC specimens are intentionally broken. With naked eye, both types of failures are estimated. As an approximation, there is 70% fiber breakage and 30% fiber pull-out. More breakage of jute fiber is due to their low tensile strength. Table 4.1 shows the compressive strength (f_c), strain (δ), energy absorption, and toughness's of PC and JFRC. It can be seen that JFRC has less f_c as compared to PC. There is decrease of 0.4 MPa in f_c of JFRC as compared to PC. However, JFRC has absorbed more energy as compared to PC. Increase of 0.02, 0.17 and 0.19 MPa in the CE_m, CE_u and CE of JFRC is seen as compared to PC, respectively. This indicates the ductile behavior of JFRC. There is difference of 4.25 in the toughness of JFRC and PC. Figure 4.1 (c) shows the comparison of compressive strength (f_c), energy absorption, and toughness's of PC and JFRC. The value of PC is taken as reference. There is only 6% reduction in the compression strength of JFRC as compared to PC. Furthermore, this point should be kept in mind that strength is not targeted. Main emphasis is high damping and impact resistance using fibers in concrete. CE_m, CE_u and CE of JFRC are increased by 2, 17 and 16 times, respectively, as that of PC. Toughness of JFRC is also enhanced by almost 4 times as that of PC.

TABLE 4.1: Compressive strength, strain, energy absorption and toughness.

Specimen	$\mathbf{f_c}$	**Strain** Δ	**Compressive Energy Absorption**			**CT**
			$\mathbf{CE_m}$ Up to $\mathbf{P_m}$	$\mathbf{CE_u}$ $\mathbf{P_m}$ to $\mathbf{P_u}$	**CTE**	
	(MPa)	**(-)**	**(MPa)**	**(MPa)**	**(MPa)**	**(-)**
(1)	(2)	(4)	(5)	(6)	(7)	(8)
PC	7.1±0.2	0.013±0.005	0.012±0.001	0	0.012±0.001	1±0.05
JFRC	6.7±0.2	0.08±0.005	0.04±0.005	0.17±0.005	0.21±0.005	5.25±0.05

Note: An average of three readings are taken.

4.2.2 Split-tension Strength, Behavior and Energy Absorption

Figure 4.2 (a) shows the behavior of specimens and developments of cracks during the test. Split-tension load-time curves for PC and JFRC are shown in Figure 4.2 (b). At 100% the maximum load of PC, first crack is developed and specimen is split into two pieces without any time. However, in case of JFRC, first crack is seen at 92% of the maximum load. Crack in JFRC is very tiny in both width and length and the specimen did not split into pieces. Number and size of cracks increases at maximum load for JFRC. Now the crack length reaches to 50 mm.

However, at ultimate load, JFRC has only observed increase in cracks numbers and sizes but still specimen is unbroken. Now the crack length is up to 70 mm. Better performance of JFRC is due to the bridging of jute fibers. JFRC specimens are intentionally broken to know the fiber's failure mechanism. With naked eye, both types of failures are estimated. As an approximation, there is a ratio to 70:30 in the fiber breakage and pull-out. Low tensile strength of jute fibers resulted in their more breakage but more bond strength has prevented them from pull-out.

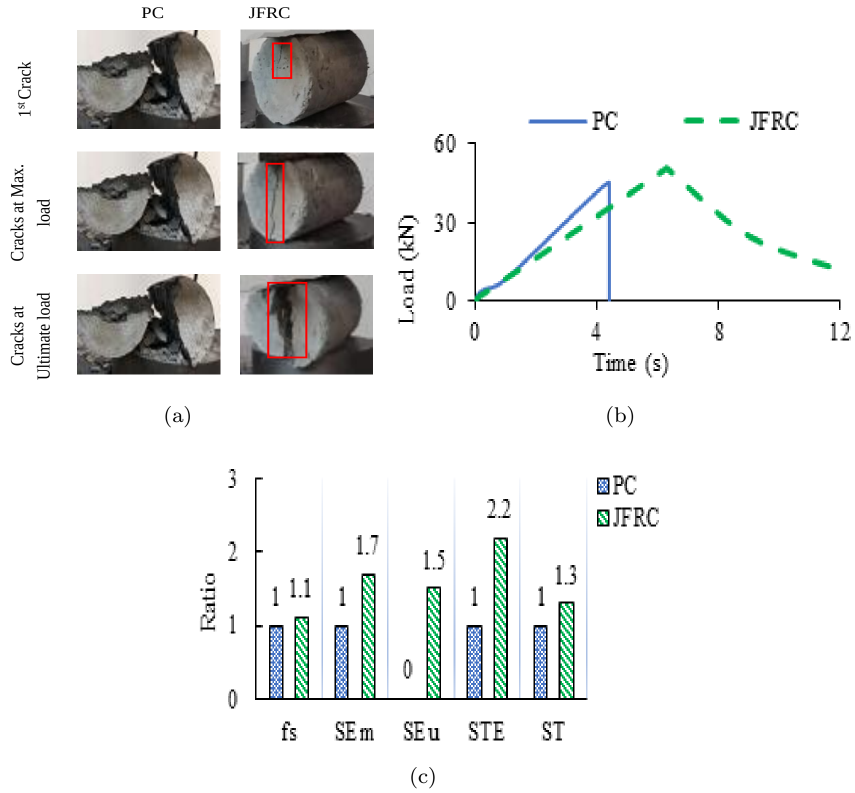

FIGURE 4.2: a) Split-tension cracking behavior, b) split load-time curve and c) split-tension strength, energy absorption and toughness index ratios.

Table 4.2 shows the split-tension strength (f_s), energy absorption, and toughness's of PC and JFRC. It can be seen that JFRC has more f_s as compared to PC. JFRC has 0.2 MPa more f_s than PC. This is because of the binding effect of JF. Furthermore, JFRC has absorbed more energy as compared to PC. SEm, SEu and SE of JFRC are increased up to 65, 56 and 120 KN.s, respectively, as compared to PC. Toughness of JFRC is increased up to 0.3 only as compared to PC. Comparison of split-tension strength (f_s), energy absorption, and toughness's of PC and JFRC is shown in Figure 4.2 (c). The value of PC is taken as reference. 1.7, 1.5 and 2.2

TABLE 4.2: Split-tension strength, energy absorption and toughness.

Specimen	**f_c**	**Split-tension Energy Absorption**			**ST**
		SE_m Up to P_m	**SE_u P_m to P_u**	**STE**	
	(MPa)	**(kJ)**	**(kJ)**	**(kN.s)**	**(-)**
(1)	(2)	(3)	(4)	(5)	(6)
PC	1.4±0.1	98±5	0	98±5	1±0.05
JFRC	1.6±0.2	162±8	56±4	218±6	1.3±0.05

Note: An average of three readings are taken.

times SE_m, SE_u and SE of JFRC are increased, respectively, as compared to PC. 1.3 times increment is also seen in the toughness of JFRC as compared to PC.

4.2.3 Flexure Strength, Behavior and Energy Absorption

Figure 4.3 (a) shows the load-deflection curves for PC, PRC, JFRC and JFSRC. Behavior of specimens and developments of cracks are presented in Figure 4.3 (b). PC specimen is split into two pieces at the maximum load right after the development of first crack. However, JFRC has observed first crack at 94% of the maximum load. At the maximum load, JFRC did not split into pieces and keeps on taking load. But now width of crack is 30 mm and it starts propagating towards top surface. Even at the ultimate load, specimen is still sound. Width of crack now reaches to 50 mm at bottom surface but top surface is intact. In case of PRC and JFSRC, first crack is seen at 80% and 72% of the maximum load, respectively. Crack in JFSRC are very tiny in both width and length as compared to the crack in PRC. At the maximum load, the crack length reaches to 50 mm and 20 mm in PRC and JFSRC, respectively. At the ultimate load, cracks length and width increased in PRC and some pieces of concrete are fallen from the specimen from the bottom side.

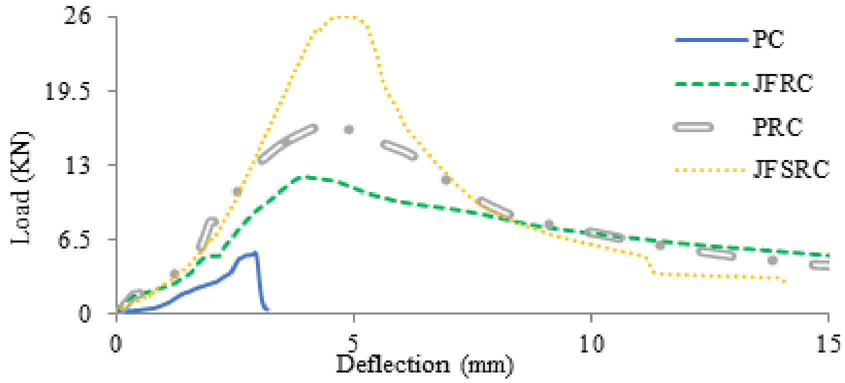

(a)

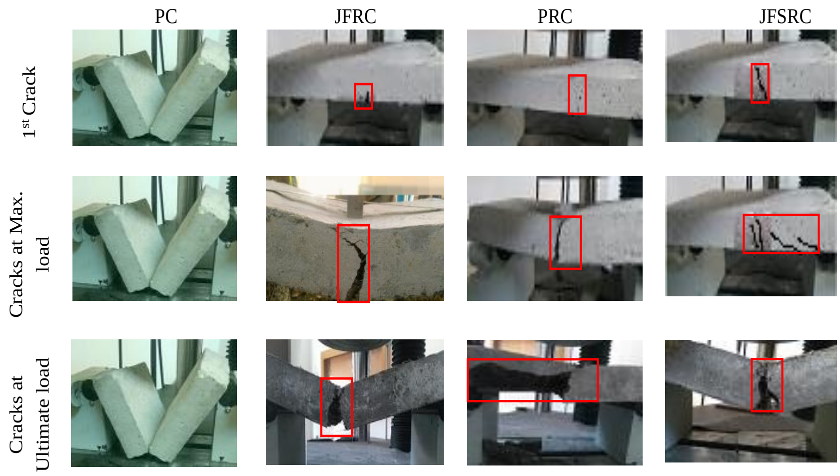

(b)

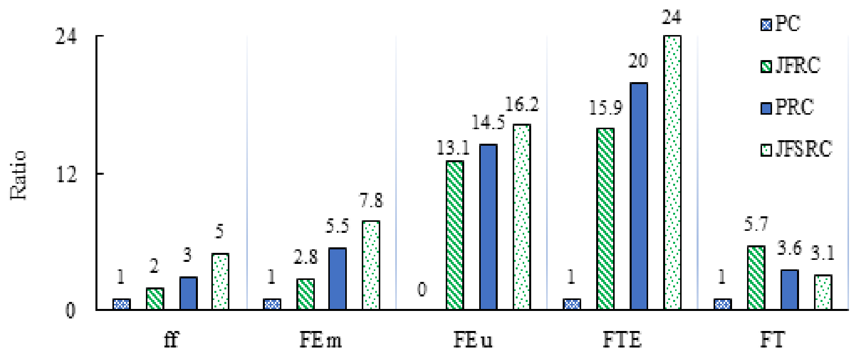

(c)

FIGURE 4.3: a) Flexure load-deflection curve, b) flexure cracking behavior and c) flexure strength, energy absorption and toughness index ratios.

But in case of JFSRC, only increase in the length and width of crack is observed. Specimen is still intact and not a single fragment of concrete is fallen. Now the crack width is up to 70 mm in JFSRC. Better performance of JFRC as compared to PC and JFSRC as compared to PRC is due to the bridging of jute fibers. Jute fibers developed a good bond within concrete matrix and no piece of concrete fell. To know the fiber's failure mechanism, JFRC specimens are intentionally broken. Fiber breakage and pull-out are evident from the broken surface. With naked eye, both types of failures are estimated. As an approximation, 70% of the fibers are broken ad 30% are pulled out. Fiber breakage is due to their low tensile strength. Flexure strength (f_s) and corresponding deflection, energy absorption, and toughness of PC, PRC, JFRC and JFSRC in Table 4.3. Improvement in the f_s of concrete is observed by the incorporation of reinforcement (either jute fiber or steel rebars). While comparing JFRC with PC, it can be seen that its f_s is increased by 2.3 MPa which is 200% increment. There is an increment of 3.2 MPa in f_s of JFSRC as compared to PRC. This indicates the better bonding and reinforcing effect of jute fibers. PRC, JFRC and JFSRC have shown better results in term of energy absorption and toughness as compared to PC. PC specimen broke into pieces at maximum load, so it hasn't absorbed any energy after maximum load. FE_m, FE_u and FE of JFRC are enhanced by 16, 77, 93 kJ, respectively, as compared to PC. There is an increment of 11, 10, and 23 kJ in the FE_m, FE_u and FE of JFSRC as compared to PRC. Significant improvement in toughness of PRC, JFRC and JFSRC is also seen, which is up to 3.5, 2.2 and 1.9 as compared to PC. Figure 4.3 (c) shows the comparison of flexure strength (f_s), energy absorption, and toughness's of PC, PRC, JFRC and JFSRC. f_s of PRC, JFRC and JFSRC is improved up to 2, 3 and 5 times as compared to PC. FE_m, FE_u and FE of JFRC are enhanced by 2.8, 13.1, 15.9 times, respectively, as compared to PC. There is an increment of 2, 2, and 4 times in the FE_m, FE_u and FE of JFSRC as compared to PRC. Toughness of PRC, JFRC and JFSRC is also enhanced by 3.6, 5.7 and 3.1 times, respectively, as compared to PC.

TABLE 4.3: Flexural strength (f_f), deflection (Δ_f), energy absorption and toughness.

Specimen	f_f	Max. Deflection Δ_f	Flexure Energy Absorption FE_m Up to P_m	FE_u P_m to P_u	FTE	FT
	(MPa)	(mm)	(kJ)	(kJ)	(kJ)	(-)
(1)	(2)	(4)	(5)	(6)	(7)	(8)
PC	1.8±0.1	3.5±1	6±0.5	0	6±0.5	1±0.1
JFRC	4.1±0.2	14±5	22±2	77±3	99±5	4.5±0.5
PRC	5.8±0.3	16±5	38±4	85±5	123±9	3.2±0.5
JFSRC	9±0.5	20±5	51±5	95±6	146±11	2.9±0.5

Note: An average of three readings are taken.

4.3 Impact Resistance

Figure 4.4 (a) shows the behavior of PC, PRC, JFRC and JFSRC under impact height of 60 cm and 90 cm. It shows the scenario of specimens' failure at different stages i.e. at the first crack and at the failure. Under impact height of 60 cm, first crack in PC is developed after 40% of total blows. However, in case of JFRC, PRC and JFSRC, first crack is seen after 42%, 49% and 63% of total blows, respectively. Cracks in JFRC, PRC and JFSRC are very tiny as compared to the crack in PC (photos of first row in Figure 4.4 (a). Failure of specimens is indicated when a complete crack is developed throughout the cross section of specimen and visible by naked eye. At failure, PC specimen split into pieces however JFRC, PRC and JFSRC has only observed the increase in the width of cracks. JFRC and JFSRC have observed flexure failure as cracks are propagated in transverse direction in contrast to PRC which observed shear cracks (photos of last row in Figure 4.4 (a)).

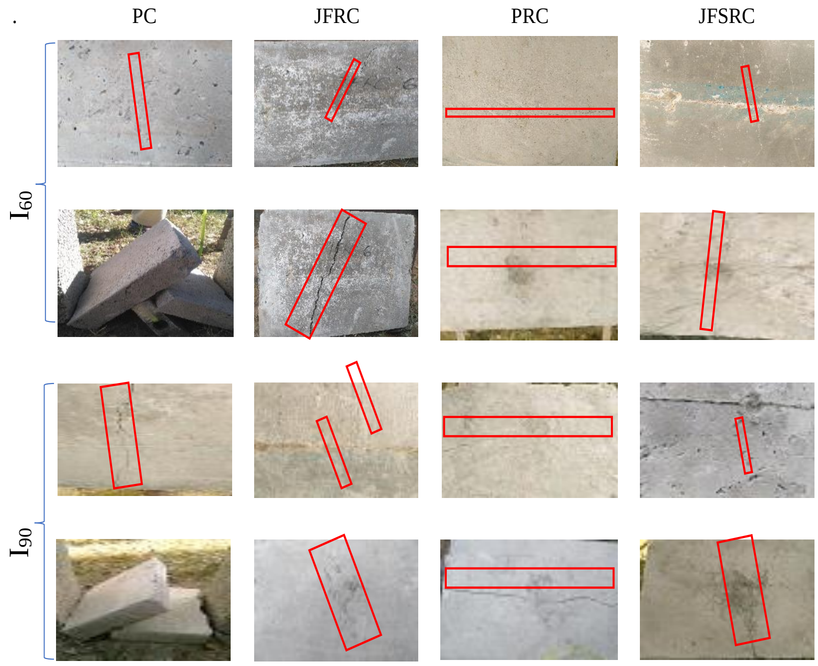

Note: I_{60} = Impact height of 60cm, I_{90} = Impact height of 90cm.

(a)

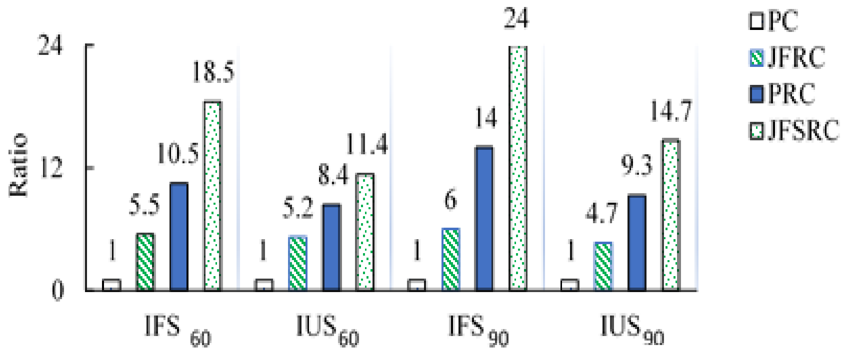

(b)

FIGURE 4.4: a) Behavior under impact test and b) comparison of impact test results.

Under impact height of 90 cm, PC observed first crack after 33% of total blows. PRC, JFRC and JFSRC have seen first crack after 48%, 41% and 53% of total blows, respectively. Very tiny cracks are seen in PRC, JFRC and JFSRC (photos of first row in Figure 4.4 (a)). PC specimen broke into pieces at failure, however, PRC, JFRC and JFSRC has witnessed increase the width of cracks. Flexure failure is seen in JFRC and JFSRC and shear in PRC (photos of last row in Figure 4.4 (a)). More blows absorbed by JFRC and JFSRC as compared to PC and PRC, respectively, are the indication of more impact resistance. Furthermore, flexure cracks also indicate the better performance of JFRC and JFSRC.

Table 4.4 shows the impact test results of different specimens when tested under different drop-weight heights. Impact first crack strength (IFS) and impact ultimate strength (IUS) of PC, PRC, JFRC and JFSRC under impact height of 60 and 90 cm are shown with their maximum deflections. IFS and IUS are presented in term of number of blows absorbed by specimens. Significant improvement in IFS and IUS of PRC, JFRC and JFSRC is observed under both impact heights as compared to PC. Under impact height of 60 cm, IFS of PC is one i.e. first crack is developed after very first blow of impact. However, in case of JFRC, PRC and JFSRC, IFS is 6, 11 and 19 blows, respectively. Ultimately, PC specimen split into pieces after 2-3 blows which means it has average IUS of 2.5 blows. Similarly, JFRC, PRC and JFSRC have average IUS of 15.5, 23.5, and 31.5 blows, respectively. Under impact height of 90 cm, PC has average IFS of 0.5 which means, some specimen broke into pieces at very first blow. However, JFRC, PRC and JFSRC have average IFS of 3.5, 7.5 and 12.5 blows, respectively. In terms of IUS, PC has average IUS of 1.5 blows. Similarly, JFRC, PRC and JFSRC have average IUS of 8.5, 15.5, and 23.5 blows, respectively.

Table 4.4: Impact test results.

Specimen	**Impact Height = 60 cm**			**Impact Height = 90 cm**		
	IFS (blows)	**IUS (blows)**	**Max. Deflection Δ_{i60} (mm)**	**IFS (blows)**	**IUS (blows)**	**Max. Deflection Δ_{i90} (mm)**
(1)	(2)	(3)	(4)	(5)	(6)	(7)
PC	1	2.5±0.5	0	0.5±0.5	1.5±0.5	0
JFRC	6.5±2.5	15.5±3.5	30±5	3.5±2.5	8.5±3.5	20±5
PRC	11.5±4.5	23.5±3.5	0	7.5±2.5	15.5±3.5	0
JFSRC	19.5±5.5	31±6	40±5	12.5±2.5	23.5±4.5	25±5

Note: 1. IFS = Impact fist crack strength, IUS = Impact ultimate strength
2. An average of five readings is taken.

It is well evident from the test results that JFSRC has maximum IFS and IUS under both impact heights. In case of JFRC, its IFS and IUS are more than PC but less than PRC. Furthermore, IFS_{60} and IUS_{60} are about 35-50% more than IFS_{90} and IUS_{90}. This indicates that impact resistance is also dependent on height/distance (or velocity) of impact force. When specimens are compared in terms of deflection, zero deflection is observed in PC as it split into two halves. In contrast to PC, JFRC has deflected up to 30 and 20 mm under impact heights of 60 and 90 cm, respectively. On the other hand, cracks are produced parallel to the longitudinal rebars in PRC due to the absence of transverse rebars. That is why, deflection in PRC is zero. But in case of JFSRC, it has maximum deflection which is up to 40 and 25 mm under impact height of 60 and 90 cm, respectively. More deflection is also the indication of flexure failure. Figure 4.4 (b) shows the comparison of impact tests results for PC, PRC, JFRC and JFSRC. The value of PC is taken as unity which is used as reference. When JFRC is compared with PC, significant improvement in impact resistance is seen. Its IFS_{60}, IUS_{60}, IFS_{90} and IUS_{90} are increased by 5.5, 5.2, 6 and 4.7 times, respectively. The increment in impact resistance is also significant when JFSRC is compared with PRC. There is an increment of about 8, 3, 10 and 5 times in the IFS_{60}, IUS_{60}, IFS_{90} and IUS_{90}, respectively.

4.4 Dynamic Properties

Table 4.5 shows different resonance frequencies, dynamic elastic modulus (E_d) and damping ratios (ξ) of different specimens. Longitudinal (f_L), transverse (f_t) and rotational (f_r) frequencies are shown for four conditions i.e. before and after flexure and impact tests. Resonance test was not possible on PC specimens for after test condition as they split into pieces. Test results presented in the Table 4.5 are average of 3-8 specimens. Results of specimens before any test are compared with the results of same specimens after flexure and impact test. It is found that there is decrease in resonance frequencies and dynamic elastic modulus but increase in damping ratios.

Table 4.5: Resonance frequencies, Dynamic Elastic Modulus and Damping Ratios.

Specimen		**Test Condition**	**No. of Specimen for average**	**Resonant Frequency**			**Dynamic Elastic Modulus, E_d**	**Damping Ration ξ**
				f_L (Hz)	**f_t (Hz)**	**f_r (Hz)**	**(Gpa)**	**(%)**
(1)	(2)	(3)	(4)	(5)	(6)	(7)	(8)	(9)
Cylinder	PC	Before Test	6	8804±350	5430±150	5499±250	30±2	2±0.5
	JFRC		6	7221±225	4290±300	7719±600	18±3	3±0.5
Slab	PC		8	4725±150	3975±250	4325±200	45±3	2±0.5
	JFRC		8	3690±200	2774±110	3195±400	76±5	4±0.5
	PRC		8	4215±200	4455±150	4655100	80±4	2±0.5
	JFSRC		8	3024±175	4009±200	3403±300	88±5	2±0.5
	JFRC	After Flexure Test	3	1287±30	1331±70	3551±160	1.5±0.3	17±2
	PRC		3	1464±50	1198±60	1642±100	2.1±0.2	16±2
	JFSRC		3	577±30	1731±150	1686±150	0.4±0.1	18±2
	JFRC	After Impact Test	5	2985±150	4527±200	1997±120	2.7±0.3	7±1
	PRC		5	3467±200	2086±150	2796±200	4.2±0.3	10±1
	JFSRC		5	754±60	1287±80	665±25	0.6±0.2	14±1

Note: f_L = Longitudinal frequency, f_t = Transverse frequency, f_r = Rotational/torsional frequency

When specimens are compared with each other in before test condition, JFRC has more E_d than PC and JFSRC has more E_d than PRC. There is an increase of 31 GPa in the E_d of JFRC as compared to PC and 8 GPa in the E_d of JFSRC as compared to PRC. Similarly, when specimens are compared in terms of damping ratios, JFRC has more damping ratio as compared to PC. It is 1% more in case of cylinder and 2% in case of slab. When specimens are examined after flexure and impact test, their E_d decreased drastically. E_d of JFRC, PRC and JFSRC are decreased up to 74, 78, 87 GPa, respectively, after flexure test. There is also a decrement of 73, 76, 87 GPa in the E_d of JFRC, PRC and JFSRC, respectively, after impact test. Hence, we can say that there is almost 98% decrement in the E_d of JFRC, PRC and JFSRC after any test. Out of all specimens, JFSRC has observed maximum decrement in the E_d.

When specimens are compared with each other, PRC has more E_d as compared to JFRC and JFSRC. In contrast to the E_d, damping ratios are increased when specimens are examined after impact and flexure test. JFRC, PRC and JFSRC have observed an increase of 23, 14, 16%, respectively, in the damping ratio when examined after flexure test. When specimens are examined after impact test, there is very less increase in damping ratios of all specimens as compared to after flexure test condition. Damping ratio of JFRC, PRC and JFSRC are increased up to 1, 8, 12%, respectively, after impact test as compared to before test condition. When specimens are compared with each other in after impact test condition, JFSRC has more damping ratio as compared to PRC. Similarly, JFSRC has also observed maximum increase in damping ratio when examined after impact test as compared to before test condition.

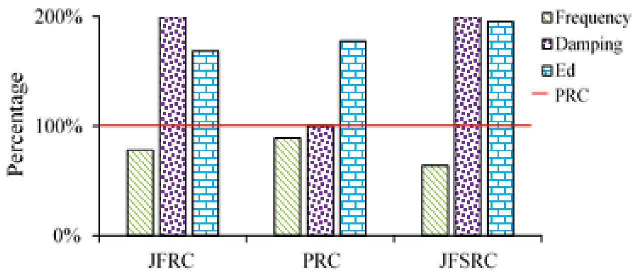

FIGURE 4.5: Comparison of longitudinal frequency, damping and dynamic elastic modulus in before test condition.

Figure 4.5 shows the comparison of longitudinal frequency, damping and E_d of PRC, JFRC and JFSRC in before test condition. The value of PC is taken as reference and it is shown as red line. Frequency decreased in all specimens and the maximum decrement is observed in JFSRC. In terms of damping ratio, JFRC and JFSRC have observed increment. Their damping ratios are double as compared to PC and PRC. Decrease in frequency and increase in damping of FRC is also reported by Giner et al. (2012). Similarly in case of E_d, JFSRC has the maximum increment as compared to PC. E_d of JFRC is enhanced by 68% as compared to PC.

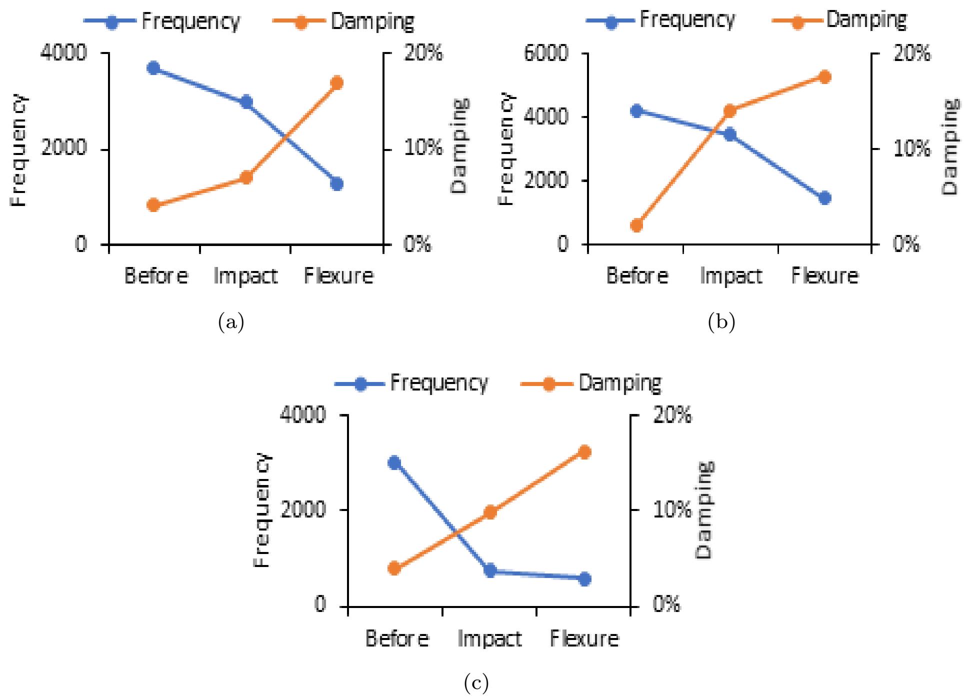

FIGURE 4.6: Trend of longitudinal frequency and damping ratio in before and after test conditions for: a) JFRC, b) PRC and c) JFSRC.

Figure 4.6 (a) show the trend of longitudinal frequency and damping for JFRC in three conditions i.e. before test, after impact and after flexure test. It can be noted that frequency and damping have inverse relation. Frequency tends to decrease when tested after any test and damping tends to increase. Similarly trend of frequency and damping for PRC is presented in Figure 4.6 (b). Damping also increased after impact and flexure test as compared to before test condition and frequency decreased. Similar trend is observed in JFSRC and it is shown in Figure

4.6 (c). While comparing damping, degree of damage of specimens should be kept in mind because more damage will lead to more damping.

4.5 SEM Analysis

Figure 4.7 shows the SEM images at failure surface of tested JFRC specimen under compressive, split-tension and flexure load. Fiber and concrete matrix interfacial bonding is studied through these images. Failure surface of tested JFRC specimen under compressive load is shown in Figure 4.7 (a). Fiber pull-out is clearly evident from the SEM images. It can be noted that there is strong bonding of concrete matrix at the toe of the pulled-out fiber at one side of the fractured surface. On the other side, less development length is available for fiber. Similarly, proper mixing of concrete is also visible from SEM images. There are very less void and the size of the voids is also very small. No voids near fibers indicate better bonding of fiber and concrete matrix.

Figure 4.7 (b) shows the SEM images at failure surface of tested JFRC specimen under split-tension load. It can be seen that cause of failure is fiber pull-out. There is cavity at the toe of fiber. This indicates the improper bonding of fiber and concrete matrix. By clearly examining the cavity at the toe of fiber, it can be noted that this cavity is not deep. This is only a small void near fiber surface which may be left due to entrapped air. Failure surface of tested JFRC specimen under flexure load is shown in Figure 4.7 (c). Under flexure load, pull-out of fibers and splitting of fiber is observed. Due to flexure load, fiber is split into threads. Circumferential debonding of fiber is also evident from the SEM image. The cavity around fiber is not deep which indicates better bonding of fiber and concrete matrix at one side of the fractured surface. On the other side, less development length is available for fiber. We can also say that there was strong bonding of fiber and concrete matrix which is weaken due to the application of flexure load. Hence, it can be concluded that main cause of fiber under compressive, split-tension and flexure load is fiber pull-out. Furthermore, proper bonding of jute fiber and concrete matrix also exists.

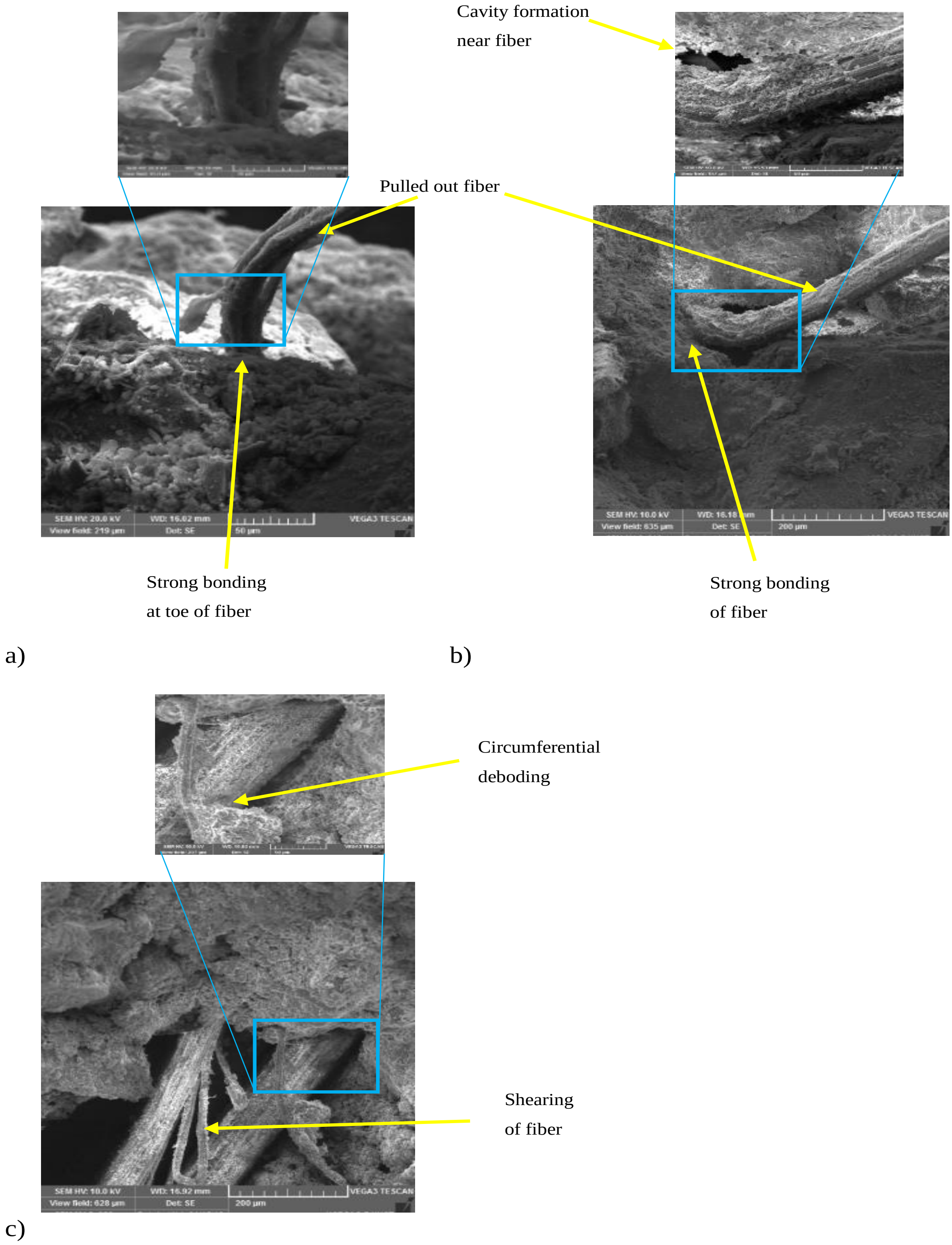

FIGURE 4.7: SEM images at failure surface of tested JFRC specimen: a) under compressive load, b) under split-tension load and c) under flexure load.

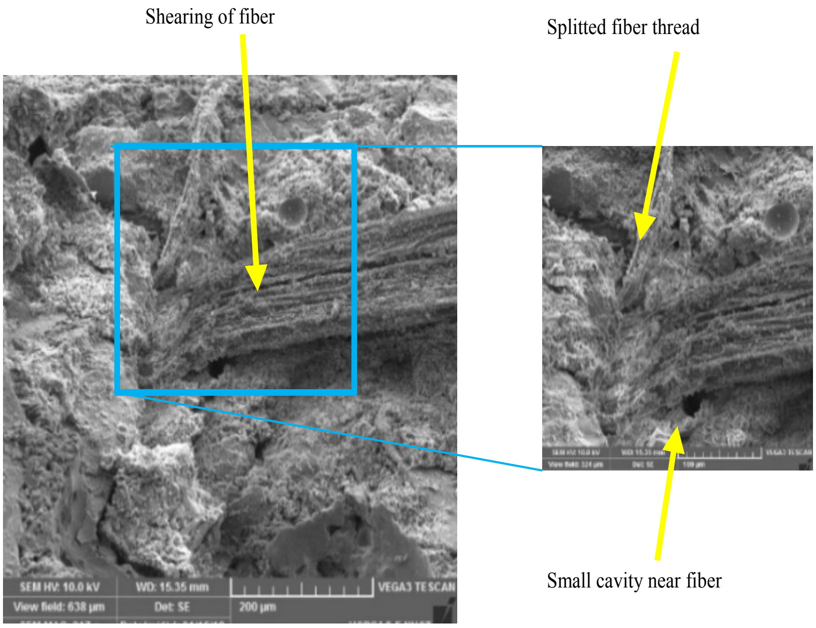

(a)

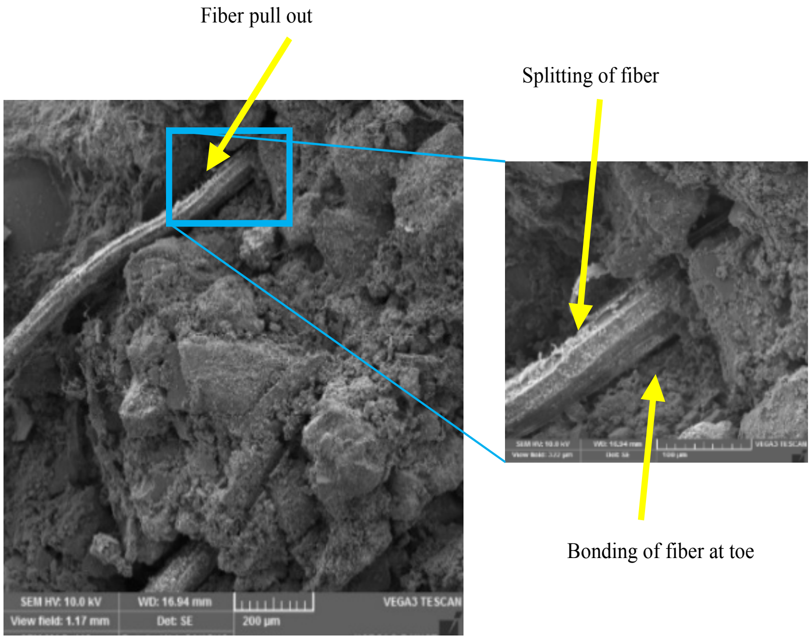

(b)

FIGURE 4.8: SEM images at failure surface of tested JFRC specimen: a) under impact$_{60}$ load and b) under impact$_{90}$ load.

Figure 4.8 shows the SEM images at failure surface of tested JFRC specimen under impact$_{60}$ and impact$_{90}$ load. Under impact$_{60}$ load, failure occurred right at the center of fiber and shearing of fiber is observed. Small thread of fiber is also splitted from it and can be seen easily. A very tiny cavity is also formed near fiber due to application of impact load. Uniformity of microstructure can also be observed from SEM images. Under impact_{90} load, fiber pull-out can be seen as cause of failure. It can be noted that splitting of small thread of fiber is also occurred which is similar to impact_{60} images. Adequate bonding of fiber with concrete matrix is also visible. A part of fiber is extended within the concrete can be seen through the cavity available at toe of fiber. Hence, we can say that splitting of fiber and cavity formation are the common aspects under both impact heights. By analyzing the SEM images at the failure surfaces of JFRC specimens, it can be concluded that fiber pull-out/splitting and cavity formation are the main flaws caused by the application of load. Adequate bonding of fiber and concrete matrix is also evident from SEM images under all loads. Furthermore, uniformity of concrete matrix can also be observed.

4.6 Summary

The mechanical properties, impact resistance and resonance frequencies of PC, JFRC, PRC and JFSRC are determined. SEM analysis of selected JFRC specimens under different loads is also performed. Increment in all mechanical properties (except compressive strength) of JFRC is observed as compared to PC. Increment of 13% and 128% in the split-tension and flexure strength of JFRC is seen. Impact resistance of JFRC is also increased up to 6 times as compared to PC. 68% and 100% increment in the dynamic elastic modulus and damping ratio of JFRC is also noticed. SEM images shows the better bonding of jute fiber with concrete matrix.

Chapter 5

Discussion

5.1 Background

The outcome of experimental testing for mechanical properties, impact resistance, resonance frequencies and failure mechanism are already explained in chapter 4. Significant improvement in the flexure strength, energy absorption and impact resistance of JFRC is observed as compared to PC. Now it's time to develop a relationship between impact resistance and mechanical properties and propose some empirical equations to predict impact resistance. Furthermore, design approach needs also to be explained.

5.2 Empirical Relationship of Impact Resistance with Mechanical Properties

Structure performance under impact loading is related to its materials properties. Concrete is the most important materials whose behavior directly affects the structure's behavior. Better performance of concrete under impact load can be related to its bending strength, toughness and energy/blows absorbed. Bending strength of concrete is normally improved by steel reinforcement. But sometimes concrete pieces starts spalling before steel failure. Hence bonding of concrete with all ingredients is also very important aspect. Better bonding of concrete matrix and enhanced concrete strength under impact load can be achieved by incorporating fiber in concrete. Furthermore, toughness can also be related to spalling as it is similar to ductility. Fibers change the concrete's brittle failure to ductile. Fibers will also help in minimizing the cracks number and size. More energy absorption will help in better post cracking behavior. Fiber are being used to increase energy absorption which in turns enhances concrete's post cracking behavior.

Empirical equations are developed with the help of obtained results from flexure test to numerically predict impact resistance. Equation are established with the help of best fit curves (refer to Figure 5.1). Empirical equations are given below:

$$IFS = 0.35 \times f_f^{1.9} \tag{5.1}$$

$$IFS = 0.2 \times FTE^{0.8} \tag{5.2}$$

$$IUS = 1.1 \times f_f^{1.6} \tag{5.3}$$

$$IUS = 0.6 \times FTE^{0.75} \tag{5.4}$$

Where IFS is impact first crack strength and IUS is impact ultimate strength in blows (for impact height of 60 cm), ff is flexure strength in MPa and FTE is flexure total absorbed energy in KJ.

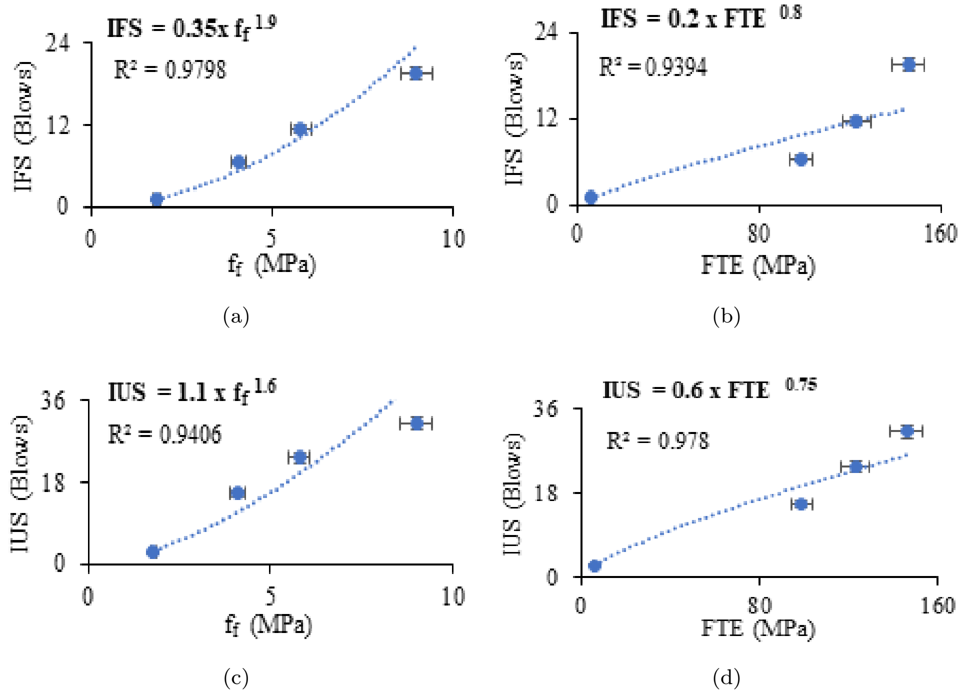

Figure 5.1: Development of empirical equations for IFS and IUS.

R^2 values and percentage error bars are also shown in Figure 5.1. It can be noted that R^2 ranges from 0.94 to 0.98 which indicates the accuracy of developed equation. It can be seen that there is very less error in the predicted equations. It is evident from the equations that there is direct relationship between impact strengths and flexure strength, energy absorption and toughness. Results from the empirical equations 4.1 to 4.4 and experimental results of IFS60 and IUS60are presented in Table 5.1. It can be seen that results from equations are very close to the experimental results for PC, JFRC PRC and JSFRC specimens. Hence, we can conclude that flexure strength and energy absorption can give better results in predicting the impact resistance of a specimen. Furthermore, we can also conclude that impact resistance is directly proportional to flexure strength and energy absorption.

Figure 5.2 shows the comparison on developed empirical equation with the experimental results. Experimental results are taken as reference and their value is taken as 100%. It can be seen that results from all equation are very near to experimental results. The difference between experimental results and proposed equations ranges from -8 to 32%. This difference is due to the variable behaviour

TABLE 5.1: Results from empirical equations and their comparison with experimental results.

Specimen	IFS (Blows)			IUS (Blows)		
	Exp.	**Eq. 5.1**	**Eq. 5.2**	**Exp.**	**Eq. 5.3**	**Eq. 5.4**
PC	1	1.1	0.8	2.5	2.8	2.3
JFRC	6.5	5.1	7.9	15.5	10.5	18.8
PRC	11.5	9.9	9.4	23.5	18.3	22.2
JFSRC	19.5	22.8	10.8	31	37.0	25.2

of different specimens under impact and flexure load. But these equations can help in predicting impact resistance for PRC and JFSRC.

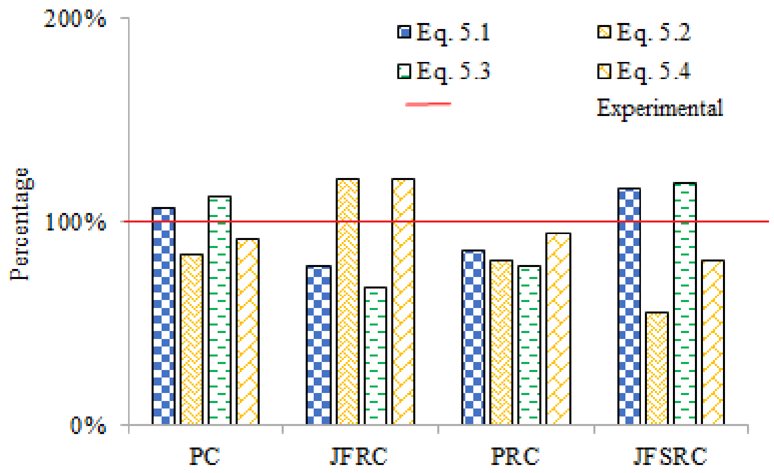

FIGURE 5.2: Comparison of results of empirical equations with experimental results.

5.3 Effect of Damping

Response of structure reduces due to the effect of damping. Hence, by increasing the damping of the structure, its motion and associated forces can be reduced. This can help in saving the steel reinforcement as it will reduce the bending moment for which the reinforcement is designed (Chopra 2001). To apply this in the design, damping of PC and JFRC is used to reduce the governing bending moment .
Damping of structure is related to the materials used. It depends upon materials

type and manufacturing process. When materials type is considered, it is related to energy losses. Hence, more energy absorption will result in more damping.

5.4 Reinforcement Design

Significant improvement in the IR of JFRC and JFSRC with respect to PC and PRC is evident from experimental results. Furthermore, flexural strength, energy absorption, dynamic elastic modulus and damping ratios are also enhanced. After confirmation of enhancement in mechanical properties from the test results, next phase is designing of slabs for impact resistance. ACI design equation cannot be used for this purpose as it ignores the effect of plain concrete in tension zone and it should not be ignored in case of FRC. Only option available is Beshara et al. equation (refer as eq. 1). But the problem with this equation is that it is for static load/moment. Equivalent static moment is found with the help of formula given by Pham and Hao (2016). Equivalent static moment is reduced by considering the effect of damping as suggested by Chopra (2001). After getting moment, Eq. 1 is used for reinforcement design of slabs. T_f used in equation 1 is tensile force of concrete in the tension zone. Its value can be found theoretically by the formula given by Beshara et al. But in this research, it is found experimentally. Maximum load taken by specimens when tested for flexure is noted. As a simplified approach, difference of loads taken by PC and JFRC specimens is computed and 50% of that value is used as T_f in Bashara's equation. Hence, the design philosophy can be simplified as: equivalent static moment is found for impact load and reinforcement is designed for that moment by considering tension zone of FRC as 50% enhanced flexural force.

PC, PRC, JFRC and JFSRC panels of size 280×432×75 mm are already tested under flexure and impact load. Maximum load taken by specimens under flexure is used while determining T_f. Moment capacities of PRC and JFSRC are calculated by using both methods i.e. ACI and Beshara et al. It is found that Beshara et al. equation gives 7% more moment capacity of specimen of same size as compared to ACI. Point to be noted is that only 50% of the enhanced flexure load is used in Beshara et al. equation and still it gives more moment capacity.

To understand the economy achieved in real situation, a slab panel of span 6 m is designed by using both methods. Design example is presented in Table 5.2. Finishes load of 1.7 kN/m^2 and live load of 2.4 kN/m^2 is assumed to be acting on slab. An impact load of 150 N is also assumed to be acting on slab. Damping of 2% and 4% is also used to reduce the moment for PC (ACI method) and JFRC (Beshara method), respectively. 50% enhanced flexure load of JFRC is used in Beshara et al. equation as T_f. ACI equation resulted 780 mm^2 of area of steel while 565 mm^2 area of steel is found from Beshara et al equation. This results in 28% saving in terms of steel reinforcement. This can only be achieved if tension zone of concrete is used in design equation. This is only possible in case of fiber reinforced concrete.

TABLE 5.2: Reinforcement design example.

Method	**Span** (m)	**Assumptions** Finishes Load (kN/m^2)	Live Load (kN/m^2)	Impact Load (N)	ξ (%)	**As Req.** (mm^2)	**As Provided** (mm^2)	**Reduction in As** (%)
ACI 318	6	1.7	2.4	150	2	762	780 (Φ10-100 mm)	-
Beshara et. al (2012)	6	1.7	2.4	150	4	565	565 (Φ12-200 mm)	28%

5.5 Summary

Relationship between impact resistance and mechanical properties are discussed and the empirical equations are developed to predict impact resistance of concrete. There is a difference of -8 to 32% in the results of empirical equations with respect to experimental results. After discussing the enhancement in the mechanical and dynamic properties of concrete, reinforcement design is also proposed by utilizing tension zone of FRC. The design approch can be simplified as: Pham and Hao (2016) formula should be used to find the equivalent static moment found for impact load and reinforcement should designed for that moment by considering tension zone of FRC as 50% enhanced flexural force. Beshara et al. (2012) equations should be used for this purpose. This will results in considerable saving of steel reinforcement in slabs.

Chapter 6

Conclusion and Future Work

6.1 Conclusion

The effectiveness of jute fibers in concrete is examined through experimental testing for improving the impact resistance and dynamic properties. Plain concrete (PC) specimens are prepared for a mix design of 1:3:2:0.7. Jute fiber, 5% by mass of cement, is added to prepare jute fiber reinforced concrete (JFRC) with same mix design. Reinforcement of Ø6@100 mm are also added in specimen to prepare plain steel rebar reinforced concrete (PRC) and jute fiber steel rebar reinforced concrete (JFSRC). A total of 52 slab panels of PC, PRC, JFRC and JFSRC are tested for flexure and impact loading. A drop-weight 1.5 kg is used to find impact resistance with drop heights of 60 and 90 cm. Twelve cylinders are tested to find the compressive and split-tension strengths. All specimens are also tested to find resonance frequencies, dynamic elastic modulus and damping ratios. Finally, reinforcement is designed for slab panel by considering tension zone of JFRC and its value is verified with experimental results. Following are the conclusions:

- Compressive strength of JFRC is only 6% less than PC. However, split-tension and flexure strengths of JFRC are enhanced by 13% and 128%, respectively, as compared to PC. Energy absorption and toughness's are increased by the incorporation of fibers in concrete. There is a minimum increment of about 220% in total energy absorption and 130% in toughness of JFRC as compared to PC.

- Significant improvement in impact resistance of JFRC is observed. 6.5 times increment for impact height of 60 cm and 6 times for impact height of 90 cm is observed as compared to PC under different types of basic loading.
- Dynamic elastic modulus and damping ratio of JFRC are enhanced by 68% and 100%, respectively, as compared to PC.
- Better microstructure of concrete matrix and interfacial bonding with fiber is seen in SEM images.
- Empirical equations are developed to predict the impact resistance with the help of mechanical properties.
- Reinforcement in slab can be minimized up to 28% by using tension zone of JFRC.

Thus, jute fiber reinforced concrete with steel rebar can be an efficient, environment friendly and economical material that is likely to be used in important structures to resist the impact load. However, before implementation, detail investigation on full structure should be done.

6.2 Future Work

Following are the recommendations for future work:

- The durability of jute fiber in concrete over a longer period in years needs to be explored.
- Impact test should also be conducted with increased drop weight.

Bibliography

ACI 318-14: *Building Code Requirements for Structural Concrete and Commentary.*

ACI 544.2R-89: *Measurement of Properties of Fiber Reinforced Concrete.*

Ali, M., Liu, A., Sou, H., & Chouw, N. (2012). Mechanical and dynamic properties of coconut fiber reinforced concrete. *Construction and Building Materials*, 30, 814-825.

Amusan, G. M., Nofiu, A. O., & Olawale S. O. A. (2017). Investigation into the Dynamic Properties of Jute Fibre Reinforced Concrete. *Journal of Scientific Research and Reports*, 15(3), 1-8

ASTM C138/C138M-16, Standard Test Method for Density (Unit Weight), Yield, and Air Content of Concrete, *ASTM International, West Conshohocken, PA*, 2016, http://www.astm.org.

ASTM C143/C143M-15a, Standard Test Method for Slump of Hydraulic-Cement Concrete, *ASTM International, West Conshohocken, PA*, 2015, http://www.astm.org.

ASTM C39/C39M-15a, Standard Test Method for Compressive Strength of Cylindrical Concrete Specimens, *ASTM International, West Conshohocken, PA*, 2015, http://www.astm.org.

ASTM C496/C496M-11, Standard Test Method for Splitting Tensile Strength of Cylindrical Concrete Specimens, *ASTM International, West Conshohocken, PA*, 2004, http://www.astm.org.

ASTM C293 / C293M-16, Standard Test Method for Flexural Strength of Concrete (Using Simple Beam With Center-Point Loading), *ASTM International, West Conshohocken, PA*, 2016, www.astm.org

Atahan, H. N., Pekmezci, B. Y., & Tuncel, E. Y. (2012). Behavior of PVA fiber-reinforced cementitious composites under static and impact flexural effects. *Journal of Materials in Civil Engineering*, 25(10), 1438-1445.

Aziz, M. A., & Mansur, M. A. (1988). Jute Fibre Reinforced Concrete Materials For Building Construction. *IABSE Congress Report*, 13.

Beshara, F. B., Shaaban, I. G., & Mustafa, T. S. (2012). Nominal Flexural Strength of High Strength Fiber Reinforced Concrete Beams. *Arabian Journal for Science and Engineering*, 37(2), 291-301.

Beckmann, B., Hummeltenberg, A., Weber, T., & Curbach, M. (2012). Strain Behaviour of Concrete Slabs under Impact Load. *Structural Engineering International*, 22(4), 562-568.

Chakraborty, S., Kundu, S. P., Roy, A., Basak, R. K., Adhikari, B., & Majumder, S. B. (2013). Improvement of the mechanical properties of jute fibre reinforced cement mortar: a statistical approach. *Construction and Building Materials*, 38, 776-784.

Chandar, S. P., and Balaji, C. J. (2015). Experimental Study on The Mechanical Properties of Concrete Mixed With Jute Fiber and Steel Fiber.*International Research Journal of Engineering and Technology*, 2, 77-82.

Chopra, A. K. (2001). *Dynamics of structures: Theory and applications.*

Eftekhari, M., & Mohammadi, S. (2016). Multiscale dynamic fracture behavior of the carbon nanotube reinforced concrete under impact loading. *International Journal of Impact Engineering*, 87, 55-64.

Giner, V. T., Baeza, F. J., Ivorra, S., Zornoza, E., & Galao, O. (2012). Effect of steel and carbon fiber additions on the dynamic properties of concrete containing silica fume. *Materials & Design*, 34, 332-339.

Gopalaratnam, V. S., Shah, S. P., Batson, G., Criswell, M., Ramakishnan, V., & Wecharatana, M. (1991). Fracture toughness of fiber reinforced concrete. *ACI Materials Journal*, 88(4), 339-353.

Hrynyk, T. D., & Vecchio, F. J. (2014). Behavior of steel fiber-reinforced concrete slabs under impact load. *ACI Structural Journal*, 111(5), 1213.

Khan, M., & Ali, M. (2016). Use of glass and nylon fibers in concrete for controlling early age micro cracking in bridge decks. *Construction and Building Materials*, 125, 800-808.

Kundu, S. P., Chakraborty, S., Roy, A., Adhikari, B., and Majumder, S. B. (2012). Chemically modified jute fibre reinforced non-pressure (NP) concrete pipes with improved mechanical properties. *Construction and Building Materials*, 37, 841-850.

Liu, B., Zhang, L. Z., Liu, Q. X., and Ji, T. (2013). Study on behaviors of jute fiber reinforced cement based materials. *Applied Mechanics and Materials*, 253, 508-511.

Mao, L., & Barnett, S. J. (2017). Investigation of toughness of ultra-high-performance fiber reinforced concrete (UHPFRC) beam under impact loading. *International Journal of Impact Engineering*, 99, 26-38.

Muda, Z. C., Usman, F., Syamsir, A., Yang, C. S., Mustapha, K. N., Beddu, S., & Itam, Z. (2016, March). Effect of Thickness and Fibre Volume Fraction on Impact Resistance of Steel Fibre Reinforced Concrete (SFRC). *In IOP Conference Series: Earth and Environmental Science*, 32(1).

Pham, T. M., & Hao, H. (2016). Prediction of the impact force on reinforced concrete beams from a drop weight. *Advances in Structural Engineering*, 19(11), 1710-1722.

Razmi, A., & Mirsayar, M. M. (2017). On the mixed mode I/II fracture properties of jute fiber-reinforced concrete. *Construction and Building Materials*, 148, 512-520.

Rehacek, S., Hunka, P., Kolisko, J., & Kratochvile, L. (2013). Two Type of Impact Load Tests, Tested on Fiber Reinforced Concrete Specimens. *Procedia Engineering*, 65, 278-283.

Saw, S. K., Akhtar, K., Yadav, N., & Singh, A. K. (2014). Hybrid composites made from jute/coir fibers: Water absorption, thickness swelling, density, morphology, and mechanical properties. *Journal of Natural Fibers*, 11(1), 39-53.

Tai, Y. S., El-Tawil, S., & Chung, T. H. (2016). Performance of deformed steel fibers embedded in ultra-high performance concrete subjected to various pullout rates. *Cement and Concrete Research*, 89, 1-13.

Ueno, H., Beppu, M., & Ogawa, A. (2017). A method for evaluating the local failure of short polypropylene fiber-reinforced concrete plates subjected to high-velocity impact with a steel projectile. *International Journal of Impact Engineering*, 105, 68-79.

Ulzurrun, G. S., & Zanuy, C. (2017). Enhancement of impact performance of reinforced concrete beams without stirrups by adding steel fibers. *Construction and Building Materials*, 145, 166-182.

Wang, W., & Chouw, N. (2017). The behavior of coconut fiber reinforced concrete (CFRC) under impact loading. *Construction and Building Materials*, 134, 452-461.

Yan, L., & Chouw, N. (2014). Dynamic and static properties of flax fibre reinforced polymer tube confined coir fibre reinforced concrete. *Journal of Composite Materials*, 48(13), 1595-1610.

Yoo, D. Y., & Banthia, N. (2017). Mechanical and structural behaviors of ultra-high-performance fiber-reinforced concrete subjected to impact and blast. *Construction and Building Materials*, 149, 416-431.

Zakaria, M., Ahmed, M., Hoque, M. M., & Islam, S. (2017). Scope of using jute fiber for the reinforcement of concrete material. *Textiles and Clothing Sustainability*, 2(1), 11.

Zhou, X., Ghaffar, S. H., Dong, W., Oladiran, O., & Fan, M. (2013). Fracture and impact properties of short discrete jute fibre-reinforced cementitious composites. *Materials & Design*, 49, 35-47.

Zia, A., & Ali, M. (2017). Behavior of fiber reinforced concrete for controlling the rate of cracking in canal-lining. *Construction and Building Materials*, 155, 726-739.

Zineddin, M., & Krauthammer, T. (2007). Dynamic response and behavior of reinforced concrete slabs under impact loading. *International Journal of Impact Engineering*, 34(9), 1517-1534.

Annexure A

Results from the testing of mechanical properties (of remaining specimens)

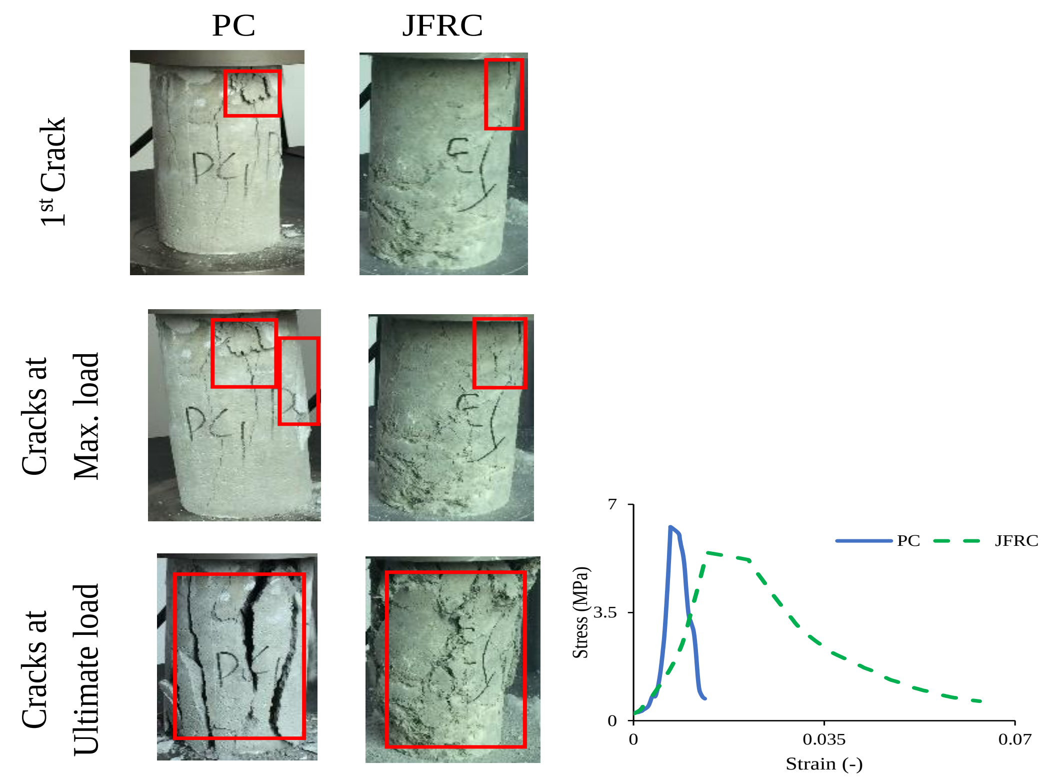

(a) (b)

FIGURE A.1: Results of compression testing: a) Cracking behavior and b) Stress-strain curve.

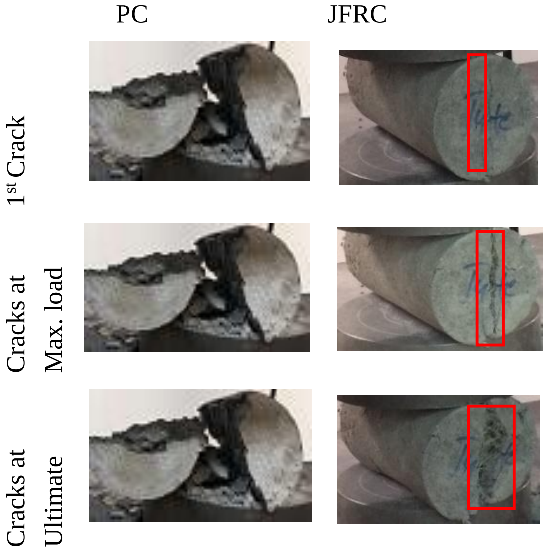

(a)

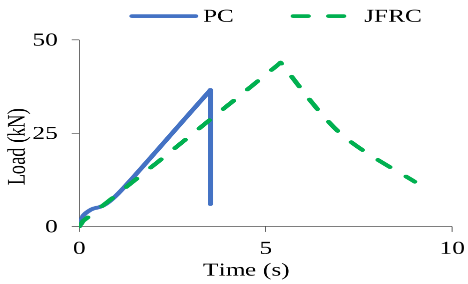

(b)

FIGURE A.2: Results of split-tension testing: a) Cracking behavior and b) Load-time curve.

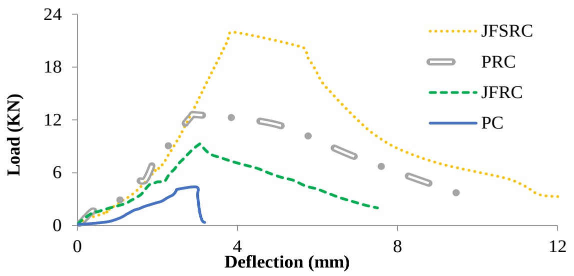

(a)

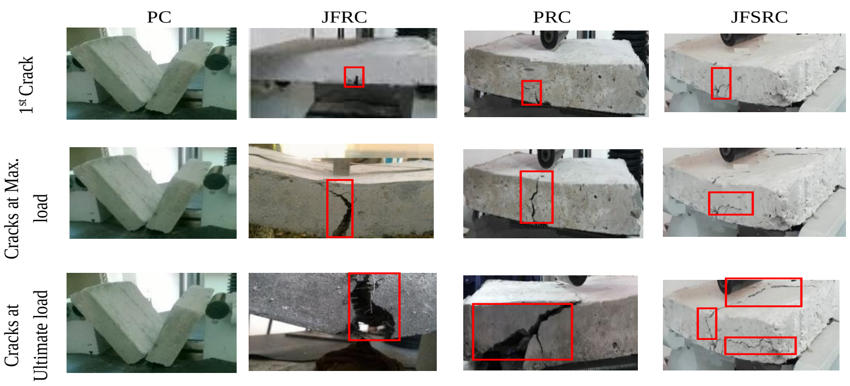

(b)

FIGURE A.3: Results of flexure testing: a) Load-deflection curve and b) Cracking behavior.

Annexure B

Results from the impact testing (of remaining specimens)

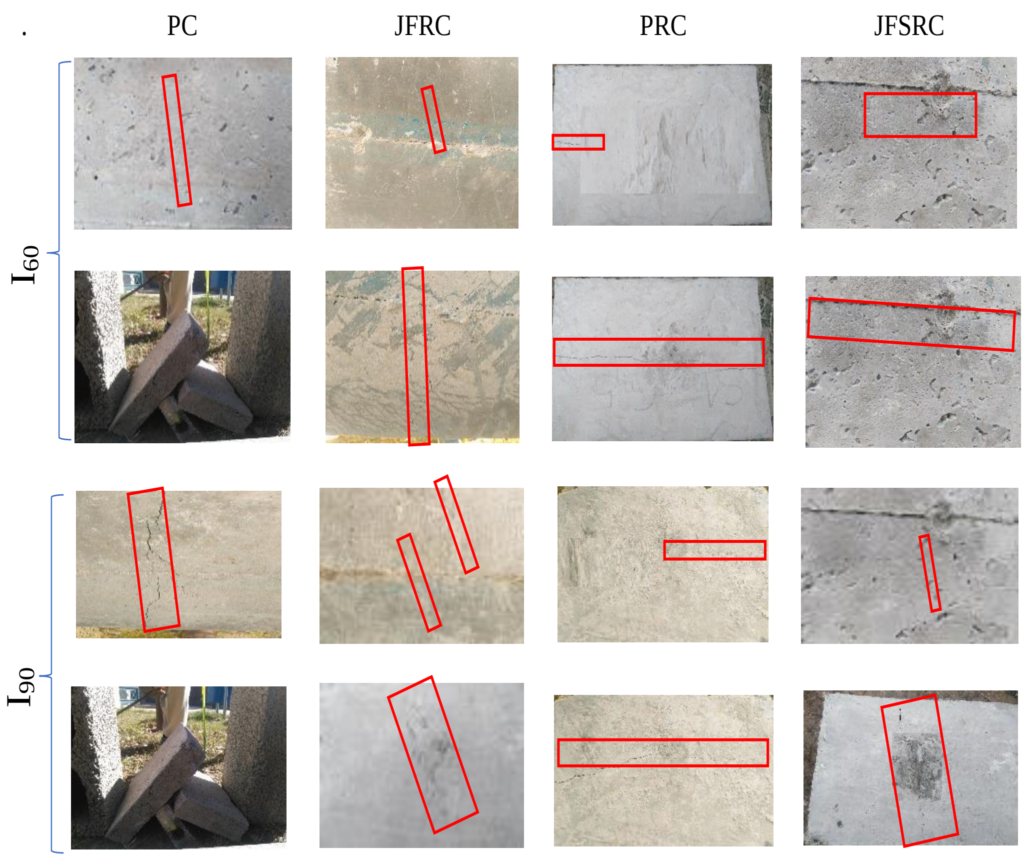

Note: I_{60} = Impact height of 60cm, I_{90} = Impact height of 90cm.

FIGURE B.1: Cracking behavior under impact load.

Annexure C

Scanning Electron Microscope Images (remaining)

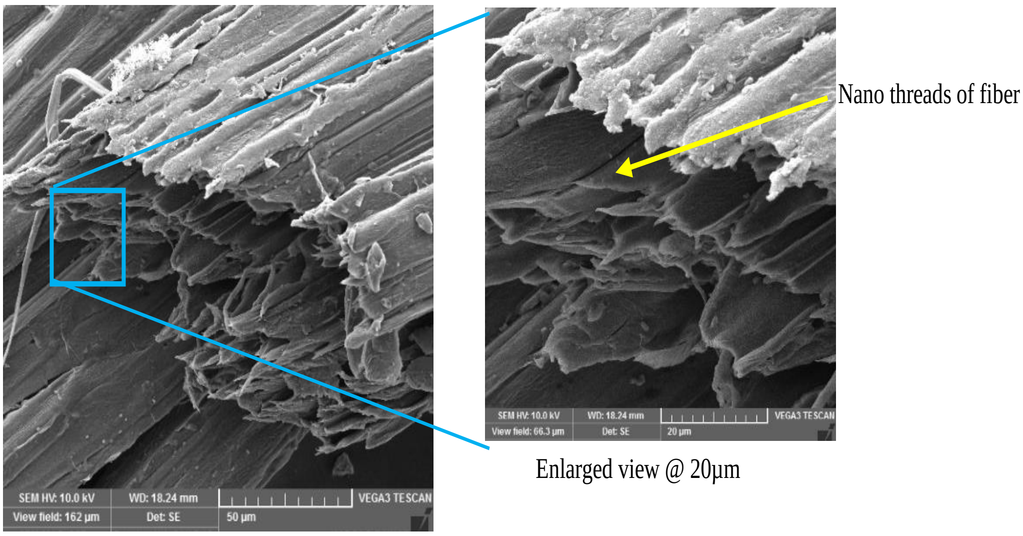

FIGURE C.1: SEM images of jute fiber.

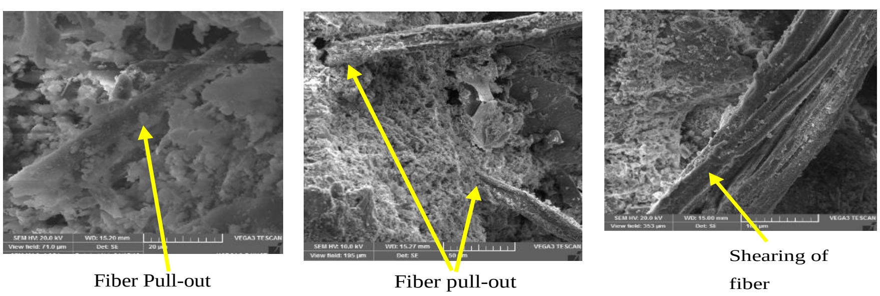

(a) (b) (c)

FIGURE C.2: SEM images at failure surface of tested JFRC specimen: a) under compressive load, b) under split-tension load and c) under flexure load.

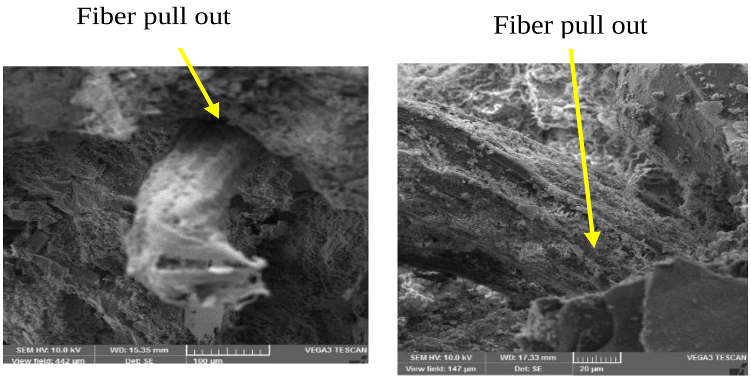

(a) (b)

Figure C.3: SEM images at failure surface of tested JFRC specimen: a) under impact$_{60}$ load and b) under impact$_{90}$ load.